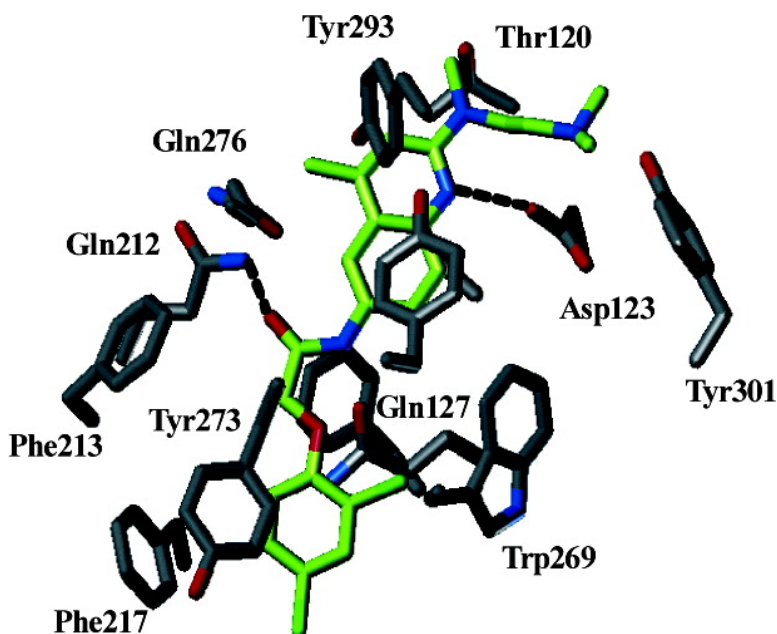


6-Acylamino-2-aminoquinolines as Potent Melanin-Concentrating Hormone 1 Receptor Antagonists. Identification, Structure–Activity Relationship, and Investigation of Binding Mode

Trond Ulven, Thomas M. Frimurer, Jean-Marie Receveur, Paul Brian Little, Ystein Rist, Pia K. Nrregaard, and Thomas Hgberg

J. Med. Chem., 2005, 48 (18), 5684-5697 • DOI: 10.1021/jm050103y • Publication Date (Web): 13 August 2005

Downloaded from <http://pubs.acs.org> on March 28, 2009



More About This Article

Additional resources and features associated with this article are available within the HTML version:

- Supporting Information
- Links to the 3 articles that cite this article, as of the time of this article download
- Access to high resolution figures
- Links to articles and content related to this article
- Copyright permission to reproduce figures and/or text from this article



Journal of
Medicinal Chemistry

Subscriber access provided by American Chemical Society

[View the Full Text HTML](#)



ACS Publications
High quality. High impact.

Journal of Medicinal Chemistry is published by the American Chemical Society, 1155
Sixteenth Street N.W., Washington, DC 20036

6-Acylamino-2-aminoquinolines as Potent Melanin-Concentrating Hormone 1 Receptor Antagonists. Identification, Structure–Activity Relationship, and Investigation of Binding Mode

Trond Ulven, Thomas M. Frimurer, Jean-Marie Receveur, Paul Brian Little, Øystein Rist, Pia K. Nørregaard, and Thomas Högberg*

7TM Pharma A/S, Fremtidsvej 3, DK-2970 Hørsholm, Denmark

Received February 2, 2005

Novel 6-acylamino-2-aminoquinoline melanin-concentrating hormone 1 receptor (MCH1R) antagonists were identified by sequential *in silico* screening with 3D pharmacophore models derived from a series of benzamide antagonists. The structure–activity relationship exploration by synthesis of analogues found structural demands around the western part of the compounds to be quite specific, whereas much structural freedom was found in the eastern part. While these compounds in general suffered from poor solubility properties, the 4-trifluoromethoxyphenoxyacetamide western appendage provided a favorable combination of activity and solubility properties. The amine in the eastern appendage, originally required by the pharmacophore model and believed to interact with Asp123 in transmembrane 3 of MCH1R, could be removed without diminishing affinity or functional activity of the compounds. Docking studies suggested that the Asp123 interacts preferentially with the nitrogen of the central quinoline. Synthesis and testing of specific analogues supported our revised binding mode hypothesis.

Introduction

Obesity has become a global epidemic with a steadily increasing prevalence not only confined to the industrialized countries.¹ Thus, the condition is no longer regarded as a cosmetic problem but a major contributor to the development of diseases including type 2 diabetes mellitus, coronary heart disease, certain forms of cancer, osteoarthritis, and sleep apnoea. Recent estimates suggest that 2–8% of the total healthcare costs in Western countries are attributable to obesity.¹ The treatment of obesity may include several approaches, including (i) reduction of food intake, (ii) prevention of fat absorption, (iii) increase of thermogenesis, (iv) modulation of fat metabolism or storage, and (v) modulation of central control of body weight, and it is reasonable to expect efficient future therapies to rely on a combination of modalities.² The increasing understanding of central control mechanisms, especially hypothalamic neuropeptide pathways, has provided novel potential targets for drug discovery.^{2,3} Thus, the orexigenic peptides agouti-related protein (Agrp), neuropeptide Y (NPY), melanin-concentrating hormone (MCH),⁴ ghrelin, and endocannabinoids have been implicated in food intake and energy homeostasis.³

MCH is a nonadecapeptide found in rat and human brain, expressed in particular in the lateral hypothalamus, and the evidence for involvement of MCH in feeding and body weight regulation is abundant.⁴ For example, up-regulated MCH mRNA is observed in fasting rats and in obese ob/ob rats, and food consumption is increased upon icv injection of MCH in rats.⁵ Also, deletion of the MCH gene in mice results in a lean phenotype,⁶ whereas overexpression of the MCH gene

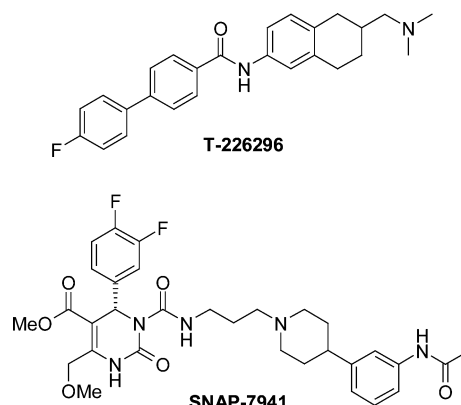


Figure 1. MCH1R antagonists.^{10,14}

in the lateral hypothalamus gives an obese and insulin-resistant phenotype.⁷ Furthermore, the hormone is reported to be involved in memory functions,⁸ anxiety,⁹ and depression.¹⁰ Two G protein-coupled seven-transmembrane (7TM) receptors, MCH1R (SLC-1) and MCH2R (SLT), have been identified for MCH, although only the former has been found in rodents.^{4,11,12} MCH1R-deficient mice are reported to be lean, hyperactive, and hyperphagic, indicating that this receptor plays a prominent role in mediating the modulatory effect of MCH on appetite and metabolism.¹³ The physiological significance of MCH2R is still unclear.

Aminotetraline T-226296 was the first reported small-molecule MCH1R antagonist,¹⁴ soon followed by SNAP-7941¹⁰ (Figure 1), and both these compounds were reported to suppress food intake induced by icv-injected MCH in rats. Furthermore, a selective peptide antagonist has been reported to reduce food intake and body weight gain after chronic administration.¹⁵ Recently, two additional compound series were reported by groups at Schering-Plough and Abbott, both with representa-

* To whom correspondence should be addressed. Phone: +45 3925 7760. Fax: +45 3925 7776. E-mail: th@7tm.com.

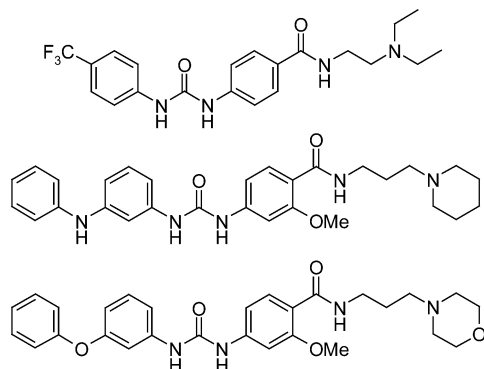


Figure 2. Representative benzamide MCH1R antagonists.¹⁷

tives exhibiting efficacy in a diet-induced obese mouse model after oral administrations.¹⁶ Thus, MCH1R antagonists are potentially interesting agents for treatment of metabolic and obesity-related disorders, as well as of disorders related to depression and anxiety.

We recently disclosed the development of a series of substituted benzamides acting as MCH1R antagonists (Figure 2).¹⁷ The design of these compounds relied on the phylogenetic¹⁸ relationship of the MCH1R with certain monoaminergic 7TM receptors with respect to features in the putative binding site involved in recognition of small-molecule ligands. Thus, the benzamides were derived by incorporation of structural features from monoaminergic receptor ligands, in particular dopamine D₂ and D₃ antagonists,¹⁹ combined with the aminotetraline T-226296.¹⁴ Docking of potential ligands in an MCH1R homology model corroborated the need of a hydrophobic western side as present in the aminotetraline.²⁰ In the present paper we describe an efficient chemotype jump using this SAR knowledge to construct 3D pharmacophores that are used for *in silico* screening of commercial compound libraries and subsequent optimization of the identified quinoline compounds.²¹ It is notable that this compound series was also independently discovered by Clark and co-workers using different virtual screening approaches based on 11 compounds from the public domain.²² However, in their case the 3D pharmacophore search did not produce any hits, and the quinolines were identified by other search strategies. Devita and co-workers have also disclosed closely related quinoline derivatives.^{23a} Another class of 2-aminoquinolines MCH1R antagonists have been reported by Souers and co-workers.²⁴

We also describe the chemical optimization and structure–activity investigations of the appendages in the 2 and 6 positions of the quinoline as well as the 4-substituent. We discovered that the eastern amine, originally required by our pharmacophore models, could be removed without loss of affinity. This prompted us to carefully analyze the receptor interactions and revise our original receptor binding hypothesis.

Computational Chemistry

Pharmacophore Models and *in Silico* Screening.

Three dimensional pharmacophore models were developed by taking advantage of binding data obtained from the benzamide series containing more than 300 members exhibiting various affinities to MCH1R (Figure 2).¹⁷ The models were produced using the pharmacophore generation module HypoGen (Catalyst).²⁵ Forty-two

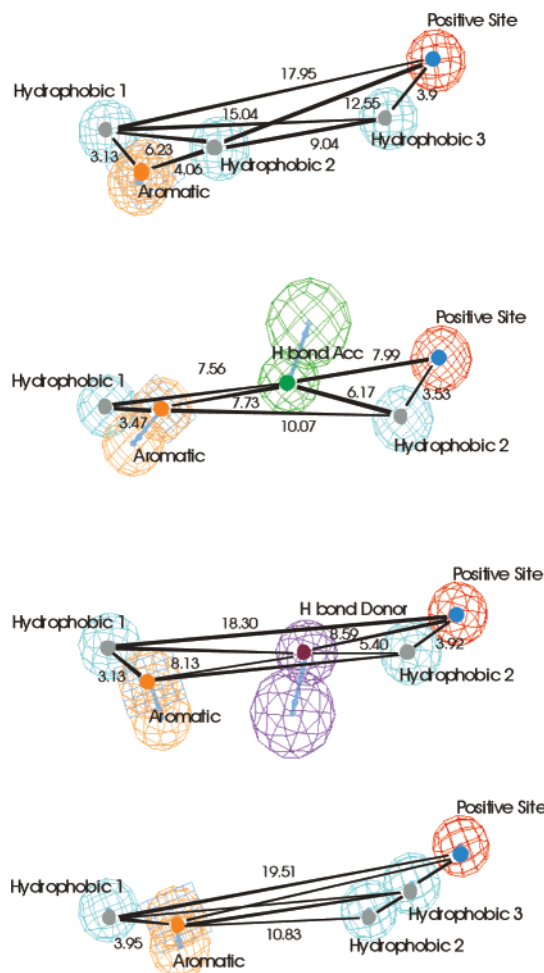


Figure 3. Four pharmacophore hypotheses on chemical features recognized by MCH1R, based on previously disclosed benzamide MCH1R antagonists.

representative benzamide MCH1R antagonists covering an affinity range of 3 orders of magnitude were used as structural input. A maximum of 255 conformers were generated for each benzamide by Catalyst's conformational search module, and the conformers were evaluated and refined by a simulated annealing protocol (see Experimental Section). Low-energy conformations of representative active MCH1R benzamide ligands served as reference structures to estimate the quality of the alignments produced by HypoGen.

Spontaneous and induced conformational changes in the protein can make a single static ligand-based pharmacophore model unable to recognize the diversity of possible binding modes induced by structurally different ligands.²⁶ Taking this into account, 25 pharmacophore hypotheses were generated, all containing four or five features, one of which was made optional. The resulting pharmacophore hypotheses were clustered into four main families, and individual models from each family were manually evaluated. The four best hypotheses, all containing five features, were chosen (Figure 3). They share a common eastern and western side, with the western side comprising a hydrophobic and aromatic feature and the eastern side comprising a hydrophobic and distal positively charged group. Apart from the spatial location of the features, the main difference

between the four hypotheses is found in a single feature in the central part.

Electronic catalogues were collected from the commercial compound suppliers, and each compound was transformed into a multiconformer library. The 3D pharmacophore models (Figure 3) were used for the in silico screening of these multiconformer libraries in a stepwise fashion. The initial small targeted library that was extracted produced 3% hits upon in vitro screening and validation. Analysis of the positive and negative information from the screening campaign was used to modify the individual weights for the pharmacophoric features. The 2-aminoquinolines were identified in the subsequent in silico search of expanded commercial libraries.

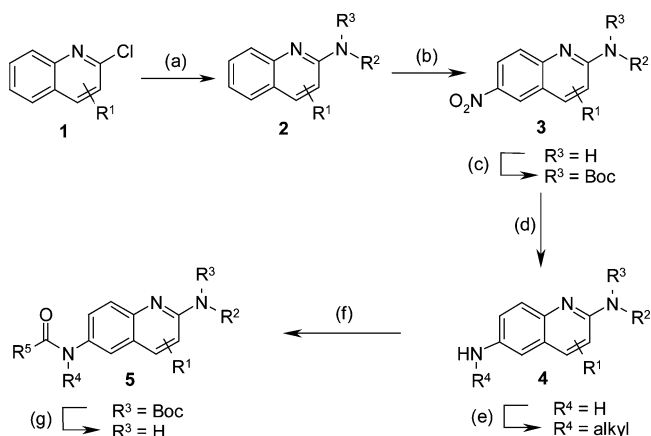
MCH1R Homology Modeling and Docking of 2-Aminoquinolines. The homology modeling study of MCH1R utilized the crystal structure of bovine rhodopsin as structural template, and the primary sequence alignment between MCH1R and bovine rhodopsin was performed on the basis of conserved residues and generic fingerprints in the TM segments. The 7TM domains of the resulting MCH1R models were superimposed onto the 7TM domain of bovine rhodopsin considering heavy backbone atoms only. The backbone rms deviation was 0.08–0.58 Å. A number of residues in the upper part of the 7TM ligand binding domain had several possible side chain conformations that could be mapped to different rotamer states. The most pronounced side chain conformational differences were observed for Asp123, Gln212, Tyr273, and Gln276, with three, four, two and four rotamer states, respectively, with less than two close contacts to other protein atoms identified for the respective residues.

Finally, the MCH1R antagonists were iteratively docked into the MCH1R model that assigned all combinatorial side chain conformations for the residues specified above. The conformations used as input structures in the docking of the MCH1R antagonists were established from a grid conformational search feature within SYBYL to locate energy minima for the torsional potential of the carbon–carbon bond at the central amide.

Chemistry

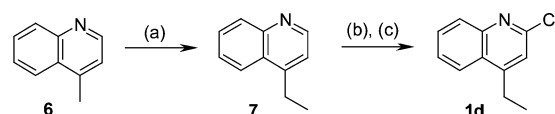
The majority of the compounds were synthesized by one of the two alternative routes shown in Schemes 1 and 4, depending on which part of the molecule represented the focus for the exploration. The 2-aminoquinolines **2** (Scheme 1) were obtained by reacting 2-chloroquinolines (**1**) with the appropriate primary or secondary amine. Exposure of **2** to cold fuming nitric acid gave the 6-nitro-2-aminoquinolines (**3**) with excellent yield and selectivity.²⁷ Reduction of the nitro group to afford **4** and coupling to the appropriate acid chloride furnished the wanted product **5**. This sequence was generally performed with excellent yields and without the need for chromatography. In the cases where primary or secondary amines were present in the side chain of **3**, these were Boc-protected prior to reduction of the nitro group, and the Boc group was removed in the final step. Analogues with N-alkylated amide ($R^4 \neq H$ in Scheme 1) were prepared by reductive alkylation of aniline **4** prior to coupling.

Scheme 1^a



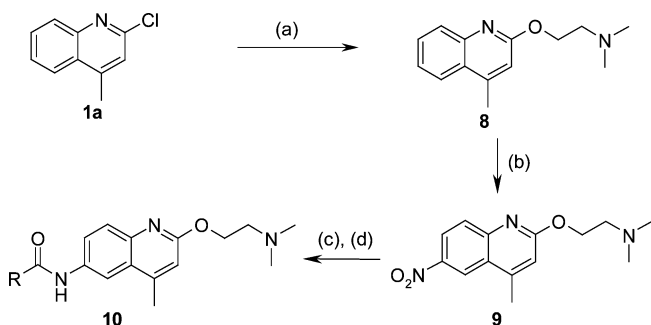
^a Reagents and conditions: (a) amine (HNR^2R^3) (2–50 equiv), neat or in EtOH or DMF, Δ ; (b) >90% HNO_3 , 0 °C, 1 h; (c) Boc₂O, Et₃N; (d) H_2 , Pd/C, THF; (e) aldehyde (R^4CHO), MeONa, MeOH, 40 °C, 2 days; then NaBH_4 , 50 °C, 2 days; (f) acid chloride (R^5COCl), CH_2Cl_2 , room temp, 3 h; (g) TFA, CH_2Cl_2 .

Scheme 2^a



^a Reagents and conditions: (a) LDA (2 M in heptane), THF, –78 °C, 90 min, then MeI, –78 °C, 2 h → room temp over 1 h; (b) mCPBA, CHCl_3 , room temp, 3 h; (c) POCl_3 , DIPEA, PhMe, 0 °C → room temp, 4 h.

Scheme 3^a

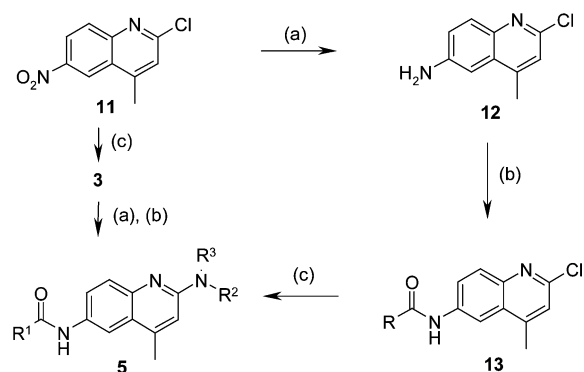


^a Reagents and conditions: (a) $\text{Me}_2\text{NCH}_2\text{CH}_2\text{OH}$, NaH, DMF, 0 °C; (b) >90% HNO_3 , 0 °C, 1 h; (c) H_2 , Pd/C, THF; (d) acid chloride (RCOCl), CH_2Cl_2 , room temp, 12 h.

The 4-ethyl analogues were synthesized from lepidine (**6**) by homologation of the 4-methyl group, N-oxidation, and treatment with phosphorus oxychloride to form 2-chloro-4-ethylquinoline **1d** (Scheme 2), which served as the substrate for the sequence shown in Scheme 1.

The 2-oxo analogues were synthesized as outlined in Scheme 3. Reaction of **1a** with dimethylaminoethoxide afforded **8**. Nitration of **8** was, as expected, less regioselective than for the 2-aminoquinolines and gave 10% of the 8-nitro isomer as a byproduct together with the desired **9**. Acylation of **9** yielded the target compounds **10**.

The sequence outlined in Scheme 1 is highly efficient for construction of libraries with diverse western parts. However, for the exploration of the eastern part, this protocol represents a four-step sequence for each compound. Thus, an alternative approach was developed using 2-chloro-6-nitroquinoline **11** as the starting point (Scheme 4).²⁸ Reduction of the nitro group by tin(II)

Scheme 4^a

^a Reagents and conditions: (a) $\text{SnCl}_2 \cdot 2\text{H}_2\text{O}$, HCl (concentrated), AcOH; (b) R^1COCl , CH_2Cl_2 , room temp, 12 h; (c) amine ($\text{R}^2\text{R}^3\text{NH}$), Δ .

chloride or by platinum-catalyzed hydrogenation afforded 6-amino-2-chloroquinoline **12**. Treatment of **12** with the appropriate acid chloride afforded the intermediates **13**, which were converted to target compounds **5** upon heating with the appropriate amine. The coupling of 2-chloroquinolines (**13**) with secondary amines was generally very efficient, whereas primary amines required harsher reaction conditions and often gave rise to byproducts from reaction with the 6-amide. However, individual tuning of temperature and reaction time frequently produced acceptable results.

Biological Evaluation

The radioligand binding assay was conducted with stably transfected Chinese hamster ovary (CHO) cells, expressing human MCH1R, by competition binding using [^{125}I]MCH. Alternatively, binding was conducted in a scintillation proximity assay (SPA) by incubating membranes and SPA beads with tracer in the presence of various concentrations of test compounds. Nonspecific binding was determined as the binding in the presence of $1\ \mu\text{M}$ MCH. Analogously, the MCH2R was expressed by stably transfected CHO cells and screened. The SPA MCH1R-membrane binding assay generally gives IC_{50} values that are up to 1 order of magnitude higher than those from the whole-cell binding assay.

The functional activity was determined in a phosphatidylinositol assay. Phosphatidylinositol turnover in stably transfected CHO cells expressing human MCH1R was stimulated by submaximal concentrations of MCH in the presence of increasing amounts of ligand. Competitive antagonism was confirmed for selected compounds by Schild analysis in a $\text{GTP}\gamma\text{S}$ SPA binding assay.

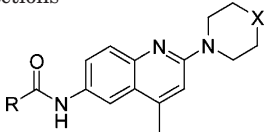
Results and Discussion

The multiconformer libraries of commercial compounds were screened in two rounds with iterative refinement of the pharmacophore models. The 375 compounds selected in the first in silico screening campaign of 0.5 million compounds resulted in 12 hits after in vitro screening and validation. None of these hits were pursued for optimization, but they provided valuable information for tuning individual weights of the four hypotheses in the query (see Supporting Information).

Out of the 411 compounds extracted in the second in silico screening campaign, which included 1.1 million commercially available compounds, 32 compounds fulfilled the hit criterion of $>80\%$ displacement of [^{125}I]MCH at $10\ \mu\text{M}$, corresponding to a hit rate of 8%. This second selection contained 42 aminoquinolines, of which 22 were classified as hits. The majority of the remaining aminoquinolines were also weak binders. The hits were tested in full dose–response curves, where six compounds, all aminoquinolines, exhibited affinities with IC_{50} values below $100\ \text{nM}$, the most potent of which was $16\ \text{nM}$ (Table 1). The quinolines coming out of this campaign all shared the common core of 6-amino-2-(1-piperazinyl)quinoline, and the compound series displayed a number of clear structure–affinity relationships.

In the eastern part, the piperazine was substituted with either *N*-methyl (**14**) or *N*-ethyl with no significant difference in the affinity of the compounds. The western parts of the compounds were structurally diverse with an aromatic ring as the common motif, preferably separated from the 6-amide by two atom linkers such as *trans*-ethenylene or methyleneoxy moieties. Out of six compounds with a shorter methylene linker between the amide and the aromatic ring, only one (**15**) displayed affinity below $1\ \mu\text{M}$. Similarly, the majority of the compounds had the aromatic ring connected directly to the amide, but only **16** exhibited high affinity, presumably because the *p*-butyl group compensates for the aromatic ring not being positioned further westward. The 5-chloro-2-methoxy motif that is favored in benzamide ligands for the related dopamine D_2 receptor only produced modest affinity (**17**), and only a *p*-methoxy (**18**) is clearly insufficient. Likewise, large annelated aromatic moieties perpendicular to the central axis of the molecule as in **19** did not pick up the same affinity as the more elongated compounds. These first results clearly suggested that separation of the aromatic ring from the 6-amide by two atoms was the preferred motif in the western part of the compounds.

The preference for the *trans*-ethenylene linker suggested that the western aromatic ring is coplanar with the quinoline system, and the 10-fold lower affinity exhibited by the saturated two-carbon linker in **20** compared to the corresponding cinnamide derivative **21** may be ascribed, at least partly, to increased conformational freedom leading to a lower population of the preferred planar conformation. A conformational search reinforced this assumption, since the preferred conformation of saturated ethylene-linked compounds adopted a planar (180°) or a perpendicular ($80^\circ/280^\circ$) arrangement of the two-carbon linker and the western aromatic ring relative to the amide quinoline. In contrast, the corresponding methyleneoxy derivatives (e.g., **26**) adopt only one clearly favored coplanar conformation (0°), where the oxygen appears to form an intramolecular hydrogen bond with the amide (see docked structures in Figure 4). This conformation was corroborated by a search in the protein–ligand crystal structure database Relibase, where seven out of eight phenoxyacetamide hits were found to adopt this exact conformation when bound to the proteins (see Experimental Section). The cinnamide derivatives were found to have two symmetrical conformations ($40^\circ/320^\circ$) quite close to the

Table 1. Representative 2-Aminoquinolines Identified in Second 3D Pharmacophore-Based and Third Scaffold Based in Silico Screening Campaigns of Commercial Compound Collections


	R	X	IC ₅₀ (nM) ^a		R	X	IC ₅₀ (nM) ^a		R	X	IC ₅₀ (nM) ^a
14		NMe	45	15		NEt	727	16		NEt	114
17		NEt	2630	18		NEt	40% ^b	19		NEt	24800
20		NEt	251	21		NEt	16	22		NMe	24
23		NMe	1800	24		NMe	47% ^b	25		NEt	41% ^b
26		NEt	22	27		NEt	95	28		NMe	438
29		NMe	52% ^b	30^c		NMe	58	31^{c,d}		NEt	442
32^c		NEt	71% ^b	33^c		NMe	224	34^c		NEt	327
35^c			41% ^b	36^c		CH ₂	82	37^c		O	56

^a SPA binding to MCH1R. ^b Single-point SPA binding to MCH1R minus % [¹²⁵I]MCH displacement at 10 μ M concentration. ^c Compounds identified in the third in silico screening campaign. ^d Connected to the quinoline core via a thioamide group instead of an amide group.

phenoxyacetamides, only about 1 kcal/mol higher than the fully extended conformation (180°), which represented the global minimum.

None of the compounds lacking the western para substituent (e.g., **23–25**) displayed impressive affinity, whereas *p*-methyl (**14**), *p*-methoxy (**21**), and *p*-chloro (**26**) exhibited high affinity. Increasing the size of the para substituent to isopropoxy (**27**) or isopentoxo (**28**) resulted in decreased affinity, suggesting that these para substituents are larger than optimal. No clear correlation between the electronic properties of the para substituent and affinity was observed. Compound **29** indicated that substitution in the meta position is forbidden, whereas compound **22** demonstrated that at least small substituents in the ortho position are allowed when combined with the methyleneoxy linker.

Following up on these promising initial hits, we conducted a scaffold-based third in silico search of commercial databases for additional compounds to complement the SAR puzzle (Table 1, footnote c).

In general, the data from the third campaign confirmed our first SAR analysis. For example, compound **30**, as expected, showed high affinity and indicated that

the *o*-chloro substituent of **22** contributes slightly to the potency. The benzylthiourea **31** exhibited lower potency than the corresponding amide analogue **20**. Constrained analogues, as exemplified by chromone **32**, were inactive. Although these compounds lack the required western para substituent, they would be expected to show a higher affinity if this modification represented an improvement. Compounds **33** and **34** demonstrated that it is possible to extend the linker to four atoms between the 6-amide and the western phenyl ring while preserving some of the affinity.

While compounds with highly diverse western parts were available from commercial sources, the same was not true for the eastern appendages of the quinolines. Only one modification preserving the eastern basic function was available, as well as a handful of modifications lacking this function. Whereas **22** represented one of the most potent hits from the initial round, compound **35** showed that replacement of the eastern methyl group with a 2-pyrimidyl led to complete loss of activity. In contrast, and initially to our surprise, some analogues of the most potent compounds lacking the distal aliphatic amine exhibited appreciable affinities (Table 1,

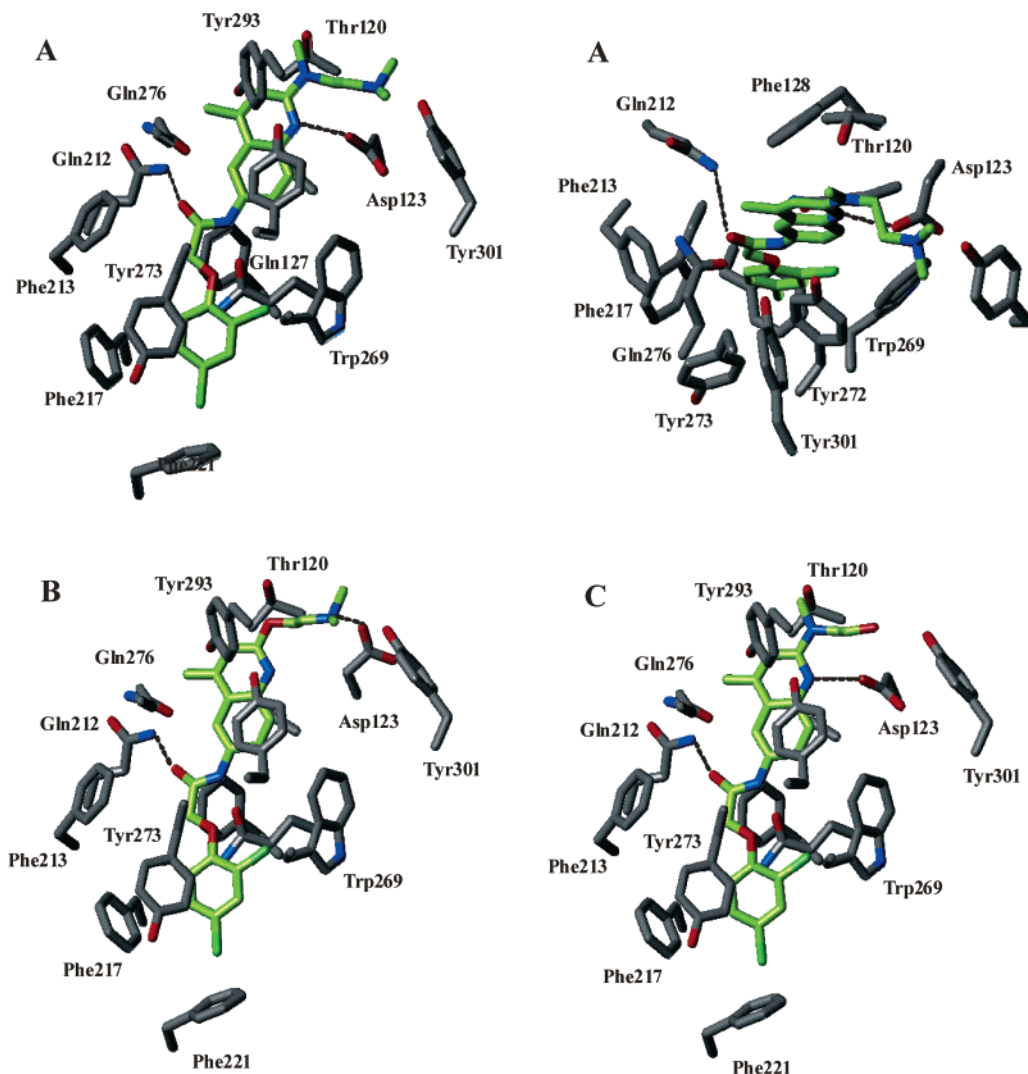


Figure 4. Binding mode of three quinolines in complex with MCH1R. The binding models differ for Asp123 on TM3, which we propose could make interactions with two accessible rotamer states depending on the ligand considered. Proposed binding site residues in contact with the ligand are shown. The residues that constitute the binding site are positioned on TM as follows: (TM3) Thr120, Asp123, Gln127, Phe128; (TM5) Gln212, Phe213, Phe217, Phe221; (TM6) Trp269, Tyr272, Tyr273, Gln276; (TM7) Tyr293, Tyr301. Ligand carbon atoms are shown in green. (A) Binding mode of **59**. In this model Asp123 ($\chi_1 = -70^\circ$, $\chi_2 = -15^\circ$) interacts with the quinoline nitrogen atom. (B) Binding mode of **65**. In this model Asp123 ($\chi_1 = -177^\circ$, $\chi_2 = 65^\circ$) interacts with the dimethylamino. (C) Binding mode of **67**. In this model Asp123 ($\chi_1 = -70^\circ$, $\chi_2 = -15^\circ$) interacts with the quinoline nitrogen atom.

bottom row). For example, piperidine analogue **36** and morpholine analogues **37** and **48** (Table 3) all exhibited affinities close to that of **22**. The redundancy of the basic amine was also noted by the Argenta group, although they found a piperidine analogue to be less potent.^{22b}

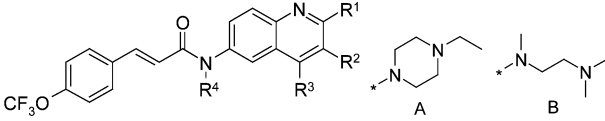
We soon realized that the compounds lacking the eastern aliphatic amine would cause serious solubility problems, and we tried to compensate for this by using a morpholine combined with the less lipophilic *p*-trifluoromethoxyphenoxymethylene western part as in **49** (Table 3), which led to very potent compounds with respect to binding and functional activity. The solubility improved for **49** (25 μM) compared to the dichlorophenoxypiperidine **36** (<5 μM) and the corresponding morpholine **48** (10 μM) but not to an acceptable level. Therefore, we decided to focus mainly on compounds in the possession of an eastern aliphatic amine function.

The initial hits all contained a 4-methyl group on their quinoline nuclei. Thus, to explore the potential for optimizing this group, we synthesized analogues with

the 4-trifluoromethoxycinnamide western part and piperazine or the more flexible dimethylaminoethyl(methyl)amine eastern side chain (Table 2). Both 4-methylquinolines **38** and **39** displayed high and similar affinity. Removal of the 4-methyl groups in **40–42** resulted in less active compounds. An even larger drop in affinity was observed when the methyl group was moved to the 3-position in **43** and **44**. Extension of the 4-methyl to 4-ethyl in **45** led to a 10-fold less active compound. On the basis of these results, we concluded that it would be difficult to optimize the 4-methyl group further.

The effect of *N*-methylating the central amide was also explored (**46**, Table 2), and this modification was found to have a pronounced negative influence on the affinity. A larger group in this position, like *N*-3,4-difluorobenzyl (**47**), led to complete loss of affinity.

At this point the structural requirements of the western and central parts of the molecule seemed relatively clear, and the attention was shifted to the eastern appendage. The optimization thus focused on

Table 2. Influence of Alkyl Substituents in the Central Part of the Molecule


	R ¹	R ²	R ³	R ⁴	IC ₅₀ WC (nM) ^a	IC ₅₀ SPA (nM) ^b
38	A	H	Me	H	2.3	16 ± 1.3
39	B	H	Me	H	16 ± 4	19 ± 4
40	A	H	H	H	29 ± 0.4	346 ± 136
41	B	H	H	H	29 ± 3	174 ± 78
42^c	B	H	H	H	20 ± 1	804
43	A	Me	H	H	50 ± 3	476 ± 176
44	B	Me	H	H	111 ± 31	1050 ± 50
45	B	H	Et	H	151 ± 40	241 ± 42
46	B	H	Me	Me	302 ± 9	1086 ± 215
47	B	H	Me	Bn ^d	5360	>10000

^a Whole-cell binding to MCH1R. ^b SPA binding to MCH1R. ^c 4-CH₃ instead of 4-CF₃O. ^d 3,4-Difluorobenzyl. Data are given as a range when $n = 2$ and as the mean ± SEM when $n = 3-4$.

compounds with the 4-trifluoromethoxyphenoxyacetamide western part, which was found to combine optimal binding properties with favorable solubility, as well as 4-trifluoromethoxycinnamide and the 4-chloro- and 2,4-dichlorophenoxyacetamide, the last two representing some of the most potent compounds from the commercial selections (e.g., **22** and **26**).

Substituting the western part of the *N*-methylpiperazine **22** with 4-trifluoromethoxyphenoxyacetamide (**50**) indeed resulted in considerably improved solubility properties as well as higher affinity (Table 3). Removal of the *N*-methyl from the eastern piperazine ring (**51**, **52** vs **22**, **26**) did not appear to influence affinity or solubility. Expansion of the piperazine ring to diazepane in **53** also had no influence on the affinity. Substitution of the piperazine ring with two methyl groups in the 3 and 5 positions (**54**) led to a considerable drop in activity, whereas introduction of a bridging methylene group in the piperazine to form a bicyclic system (**55**) seemed to increase potency and also produced acceptable solubility properties.

Introduction of 4-pyrrolidinylpiperidine in the place of the piperazine (**56**) gave equally high affinity as well as single-digit nanomolar functional antagonism. Replacement of the 4-pyrrolidine by a primary amine (**57**) produced a potent compound that appeared to have favorable solubility properties. Again in opposition to our original pharmacophore hypotheses, removal of the primary amine in **57** to produce piperidine **58** did not deteriorate potency.

As seen in Table 2, affinity was preserved upon opening of the piperazines (**38**, **40**, **43**) to form *N,N,N*-trimethylethylenediamine analogues (**39**, **41**, **44**). Correspondingly, both the affinity and antagonistic activity

of **59** paralleled what was observed for the piperazine analogue **22**. Removal of a methyl group from either the terminal (**60**) or the adjoining (**61**) nitrogen of the ethylenediamine (cf. **22** and **39**) had no impact on the activity nor did introduction of a methyl group onto the ethylene linker (**62**). Introduction of eastern *N*-ethylpyrrolidine groups (**63**) was also permitted, as was homologation to dimethylaminopropyl (**64**).

Exchange of the adjoining 2-amine functions of **39**, **59**, **61** with 2-oxy in **65** and **66** resulted in a considerable drop in both affinity and functional activity of 1–2 orders of magnitude, suggesting that the 2-amine function is important for the affinity of the compounds. On the other hand, exchange of the distal dimethylamine group of compounds **39** and **59** with a hydroxyl group (**67**, **68**) enhanced the activity but without having the same beneficial effect on solubility as the terminal amine. A terminal acetoxy group (**69**) turned out to be very similar to the terminal hydroxyl (**67**), ruling out a hydrogen bond donor interaction in the binding of the latter.

The majority of the compounds were counterscreened on the receptors MCH2R and 5-HT_{2c}, the latter as a representative of monoamine receptors displaying cross-affinity with MCH1R. Furthermore, 5-HT_{2c} is also implicated in the regulation of food intake, and 5-HT_{2c} agonists have been shown to suppress appetite.²⁹ None of the compounds displayed problematic affinities toward these receptors, and a 1000-fold or higher selectivity was found for most compounds. Two compounds (**39** and **65**) with different eastern side chains were also characterized in a broader panel of receptors and transporters with no notable differences in their profile (Table 4).

The high affinity and functional activity of the compounds lacking an eastern amine function were not anticipated by us because a positive charge in the eastern distal position was a prerequisite in all pharmacophore models. This charge was assigned to interact with Asp123, located in TM3 of MCH1R. Representative compounds were docked in a rhodopsin templated MCH1R homology model. Upon analyzing the docked quinolines in the binding site (Figure 4), we realized that rotation of the Asp123 residue could readily accommodate an interaction with the basic nitrogen in the quinoline core. This docking mode was found to be somewhat more favored than the originally anticipated interaction between the terminal aliphatic amine and the aspartate.

Figure 4A shows top and side views of the docking of **59** in MCH1R. Key interactions include a hydrogen bond between Gln212 and the amide carbonyl and between the western aromatic ring and a hydrophobic pocket formed by Phe213, Phe217, Phe221, Trp269, and Tyr273. In agreement with the SAR studies, the model accommodates a higher degree of freedom in the interaction between the eastern part of the quinolines and the upper part of the binding pocket. Two favored rotameric states were identified for Asp123 on TM3, the first ($\chi_1 = -70^\circ$, $\chi_2 = -15^\circ$) in 51% and the second ($\chi_1 = -177^\circ$, $\chi_2 = 65^\circ$) in 21% of the structures (see Experimental Section), both of which were invoked in the homology models. The low-energy conformation of the phenoxyacetamide moiety identified in the conformational grid

Table 3. Binding and Antagonistic Activity on MCH1R, Binding to MCH2R and 5-HT_{2c}, and Approximate Solubility of Representative Quinolines

	R ¹	X-Y	R ²	MCH1R			MCH2R	5HT _{2c}	Solu. (μ M) ^d
				IC ₅₀ WC (nM) ^a	IC ₅₀ SPA (nM) ^b	IC ₅₀ IP3 (nM) ^c	IC ₅₀ (μ M) ^a	IC ₅₀ (μ M) ^b	
22	2,4-Cl ₂	O-CH ₂		6.4 ± 1.4	24 ± 5	89 ± 17	>10	0.61	25
48	2,4-Cl ₂	O-CH ₂		5.5 ± 1.6	59 ± 2.3	15.4	---	---	10
49	4-CF ₃ O	O-CH ₂		1.6 ± 0.1	82 ± 10	12 ± 3	>10	>10	25
50	4-CF ₃ O	O-CH ₂		2.3	29	25	---	---	120
51	2,4-Cl ₂	O-CH ₂		5.0	16 ± 4	74 ± 8	3.7	2.0	25
52	4-CF ₃ O	CH=CH		4.0	65 ± 19	88 ± 9	>10	1.1	25
53	4-CF ₃ O	CH=CH		6.1	23	65	---	1.6	---
54	4-CF ₃ O	CH=CH		100	409	1160 ± 690	---	---	---
55	4-CF ₃ O	O-CH ₂		1.9 ± 0.4	9.7	16 ± 2	6.8	---	150
56	4-CF ₃ O	O-CH ₂		1.5 ± 0.5	7.1 ± 2.2	7.5 ± 0.3	6.3	---	---
57	4-CF ₃ O	O-CH ₂		1.5 ± 0.2	3.5	14 ± 2	4.7	---	150
58	4-CF ₃ O	O-CH ₂		0.92 ± 0.08	97	19 ± 2	---	---	---
59^e	2,4-Cl ₂	O-CH ₂		5.9 ± 2.1	9.4 ± 1.6	66 ± 3	4.5	---	80
60	2,4-Cl ₂	O-CH ₂		6.1	6.9 ± 1.0	28	6.8	0.77	100
61	4-CF ₃ O	CH=CH		3.0	13 ± 3	42	8.4	5.7	---
62	4-CF ₃ O	CH=CH		4.3	22	98	---	18	---
63	4-CF ₃ O	O-CH ₂		8.7 ± 0.7	21 ± 13	109 ± 29	>10	4.7	---
64	4-CF ₃ O	O-CH ₂		2.7 ± 1.1	3.8 ± 1.3	16 ± 2.8	7.1	4.0	---
65^e	2,4-Cl ₂	O-CH ₂		85 ± 28	180 ± 50	1480 ± 566	8.7	2.6	---
66	4-CF ₃ O	CH=CH		158 ± 40	416 ± 74	---	---	---	---
67^e	2,4-Cl ₂	O-CH ₂		2.1 ± 0.1	43 ± 14	11 ± 1	>10	5.9	5
68	4-CF ₃ O	CH=CH		0.90 ± 0.17	41 ± 12	5.2 ± 3.7	6.4	>10	---
69	2,4-Cl ₂	O-CH ₂		2.3 ± 1	29	14 ± 6	>10	---	---

^a Whole-cell binding. ^b SPA binding. ^c Inhibition of MCH-induced IP accumulation. ^d Solubility determined by addition of 10 mM DMSO solution of test compound to PBS (pH 7) until opalescence. ^e Schild analysis from [³⁵S]GTP γ S assay: **59**, $K_B = 5.0 \pm 1.0$ nM; **65**, $K_B = 76$ nM; **67**, $K_B = 3.0$ nM. Data are given as a range when $n = 2$ and as the mean \pm SEM when $n = 3-4$.

search was used in the docking of compounds **59**, **65**, and **67** into the binding site of the MCH1R, shown in Figure 4. Contrary to our original hypotheses, Asp123 appeared to preferably interact with the quinoline nitrogen rather than the aliphatic amine, which corresponded to the most abundant rotamer state. The 2-amino substituent at the quinoline is expected to increase the basicity of the quinoline nitrogen significantly, and calculated microscopic pK_a values of the quinoline nitrogen of **59** indeed predicted it to be more basic than the aliphatic dimethylamine (Figure 5).³⁰

To corroborate this binding mode hypothesis, **65** was investigated in the receptor model (Figure 4B). In this compound the electron-donating nitrogen in the 2-position of the quinoline of **59** is substituted with the electron-withdrawing oxygen, resulting in a drop in basicity of more than 4 pK_a units for the quinoline nitrogen (Figure 5). For this compound the dimethylamine was found to interact with the Asp123 in the less abundant rotameric state.

In analogue **67** (Figure 5) the electron-donating nitrogen is reinstated, whereas the aliphatic amine is

Table 4. Receptor Profiling (IC_{50} , μM) of Compounds **39** and **65** on Select Receptors

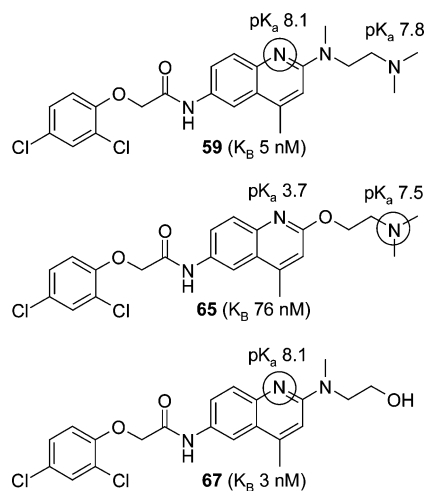
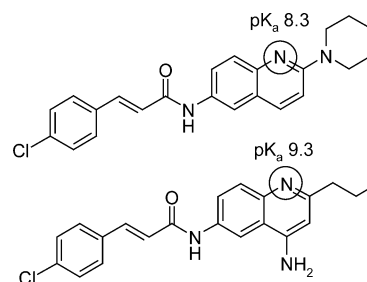
	39	65
adrenergic α_2	1.3	0.25
dopamine D_1	0.90	7.5
dopamine D_3	2.3	1.3
histamine H_1	>10	3.5
histamine H_2	0.86	0.87
muscarinic M_1	1.3	1.7
muscarinic M_2	0.48	4.5
serotonin 5-HT _{1B}	0.80	0.20
serotonin 5-HT _{2A}	1.9	0.61
serotonin 5-HT _{2C}	0.9	2.5
DA transporter	10	>10

replaced by a hydroxyl group. Docking of this compound in the MCH1R model resulted in a binding mode analogous to the one found for **59** (Figure 4C). It is noteworthy that compounds **59** and **67**, for which the quinoline nitrogen was found to be the most basic site and only differing structurally in the distal eastern end, exhibited very similar affinities and functional activities on MCH1R. On the other hand, **65** came out 1 order of magnitude less potent in the binding assays and 2 orders of magnitude less potent in the functional assay. Schild analysis confirmed the compounds to be competitive antagonists, with K_B values corresponding very well to affinities obtained in the whole-cell binding assay. These observations strengthened our confidence in the proposed new binding mode.

The structurally related 2-aminoquinoline (Figure 6, top) and the isoelectronic 4-aminoquinolines (Figure 6, bottom) disclosed as MCH1R antagonists by Devita and co-workers²³ are very likely to adopt the same binding mode in MCH1R as our quinolines. The latter compound has the 2-amine replaced by an alkyl chain, and a primary amine in the 4-position is instead responsible for enhancing the basicity of the quinoline atom, corroborating the idea that the electron-donating property of the 2-amino group is more important than any specific direct interactions with the binding site.

Conclusion

By using SAR knowledge in the construction of 3D pharmacophore models and using these for in silico screening of commercial compound collections, we accomplished our objective to move from our original benzamide series to novel MCH1R antagonists of a significantly different chemotype. Subsequent optimization of the identified 6-acylamino-2-aminoquinoline compounds furnished potent compounds with appreciable selectivity and favorable physicochemical properties. The series displayed quite specific structural demands around the western aromatic ring and the linking amide moiety. A substituent in the para position of the western phenyl ring was required, and the trifluoromethoxyphenoxyacetamide appendage provided a suitable combination of activity and solubility properties. We were unable to optimize the 4-methyl substituent found in the original 2-aminoquinoline hits. The requirements in the eastern appendage were found to be highly flexible, and this part of the molecule, when carrying an amine function, was found to serve a more important role in increasing the solubility of the compound. The eastern distal aliphatic amine implicated by the pharmacophore models turned out not to be

**Figure 5.** Competitive antagonists with different potential Asp123 interaction sites, which were docked into the MCH1R. The presumed site of interaction with Asp123 is indicated by circle on each compound, and calculated³⁰ microscopic pK_a values for the basic sites are given.**Figure 6.** Related 2- and 4-aminoquinoline derivatives reported by others to be MCH1R antagonists.²³ The presumed site of interaction with Asp123 is indicated by a circle on each compound, and calculated³⁰ microscopic pK_a values are given.

mandatory for activity. This observation was rationalized by a docking study, indicating that Asp123 in its preferred rotameric state interacts preferentially with the quinoline nitrogen instead of the aliphatic amine. This new binding mode found support in microscopic pK_a calculations as well as studies of analogues where the basicity of the quinoline site was reduced or the distal aliphatic amine was removed.

Experimental Section

General Comments. Melting points were determined on an Electrothermal 9200 melting point apparatus. ¹H and ¹³C NMR spectra were recorded on a Bruker AMX 300 spectrometer operating at 300.13 and 75.47 MHz, respectively. Spectra were calibrated relative to tetramethylsilane internal standard or residual solvent peak. High-resolution mass spectra (HRMS) were obtained on a JEOL-SX 102 in FAB⁺ mode with NBA matrix. Analytical HPLC was performed on an Agilent 1100 series instrument equipped with a UV detector and a VL mass detector operating under electrospray ionization conditions in positive (ESI⁺) or negative (ESI⁻) mode. HPLC method A1 had the following parameters: column, Waters XTerra MS C18; flow, 1.0 mL/min; gradient, 0–5 min, 15–100% acetonitrile in water; 5–7¹/₂ min, 100% acetonitrile; modifier, 5 mM ammonium formate. HPLC method A2 was the same as method A1 except for the flow, which was 0.7 mL/min. HPLC method A3 had the following parameters: column, Waters XTerra MS C18; flow, 1.2 mL/min; gradient, 0–4 min, 5–100%

acetonitrile in water; 4–6½ min, 100% acetonitrile; modifier, 0.1% ammonia. HPLC method B1 had the following parameters: column, Agilent Zorbax Eclipse XDB-C8; flow, 0.8 mL/min; gradient, 0–8 min, 20–100% acetonitrile in water; 8–10 min, 100% acetonitrile; modifier, 0.1% formic acid. HPLC method B2 had the following parameters: column, Agilent Zorbax Eclipse XDB-C8; flow, 0.8 mL/min; gradient, 0–10 min, 20–100% acetonitrile in water; 10–14 min, 100% acetonitrile; modifier, 0.1% formic acid. Elemental analyses were performed by Johannes Theiner at Mikroanalytisches Laboratorium, University of Vienna, Austria, and results are within 0.4% of the calculated values unless otherwise stated.

General Procedure I. Introduction of 2-Amine. A stirred mixture of the 2-chloroquinoline **1** (1 equiv) and primary or secondary amine (2–5 equiv) was heated (a) to 150 °C for 2 h, (b) to 100 °C for 16 h, or (c) in a sealed vessel in an Emrys Optimizer (Personal Chemistry) microwave oven to 200 °C for 15 min. Excess amine was removed in vacuo if possible. The residue was taken up in 3% aqueous HCl. The aqueous phase was washed twice with CH₂Cl₂, 4 N NaOH was added until pH 8 was reached, and the sample was extracted three times with CH₂Cl₂. The extract was concentrated to give the corresponding 2-aminoquinoline **2**, which was used directly or purified by recrystallization or chromatography, as appropriate.

General Procedure II. Nitration. 2-Aminoquinoline **2** was added in small portions to cold (–10 °C), stirring, fuming HNO₃ (>90%, 1 mL/g of **2**). The mixture was stirred at 0 °C for 1 h and then poured into an ice/water mixture. To the aqueous mixture was added 4 N NaOH until pH 12 was reached, and the mixture was left to precipitate overnight. The precipitate was filtered off, washed four times with water, and dried in vacuo to give the 2-amino-6-nitroquinoline **3**, which was purified by recrystallization or used directly in the next step.

General Procedure III. Introduction of Boc Group. To a solution of 2-amino-6-nitroquinoline **3** (1 equiv) in CH₂Cl₂ (~10 mL/g of **3**) were added Boc₂O (2 equiv) and Et₃N (1 equiv), and the mixture was stirred at room temperature for 12 h. The mixture was poured into water and was extracted three times with CH₂Cl₂. The extract was dried (MgSO₄) and concentrated to give to give the corresponding Boc-protected compound.

General Procedure IV. Reduction of Nitro Group. A mixture of 2-amino-6-nitroquinoline **3** and 5% Pd/C (~200 mg/g of **3**) in THF or ethanol was stirred under hydrogen (1 atm) for 12 h. The reaction mixture was filtered over a pad of Celite and concentrated in vacuo to give the 6-aminoquinoline **4**, which was purified by chromatography or recrystallization or used directly in the next step.

General Procedure V. Coupling of Aniline with Acid Chloride. To the 6-aminoquinoline **4** (1 equiv) in dry CH₂Cl₂ was added a solution of the acid chloride (1.1 equiv) in dry CH₂Cl₂. The resulting mixture was stirred for 3 h. The mixture was diluted with CH₂Cl₂, washed with 1 N NaOH and brine, dried (MgSO₄), and concentrated. The crude product was purified by recrystallization or chromatography.

General Procedure VI. Removal of Boc Group. To the Boc-protected compound in CH₂Cl₂ (15 mL/g of substrate) was added trifluoroacetic acid (1.5 mL/g of substrate), and the mixture was stirred at room temperature for 12 h. The reaction mixture was concentrated, and the residue was partitioned between aqueous Na₂CO₃ and EtOAc. The aqueous phase was extracted with EtOAc, and the combined organic phases were dried (MgSO₄) and concentrated. The residue was purified by flash chromatography.

General Procedure VII. Acylation of 6-Amino-2-chlorolepidine. To 6-amino-2-chloro-4-methylquinoline **12** (1 equiv) in dry CH₂Cl₂ (5 mL per mmol) was added dropwise or in small portions the acyl chloride (1 equiv). The mixture was stirred at room temperature for 2 h, then poured into MeOH (15 mL per mmol) to give a homogeneous solution. Water (10 mL per mmol) was added in small portions, and the mixture was left to precipitate. The crystals were collected and washed

with MeOH/water (1:1). The filtrate was concentrated, and additional crops of crystals were collected if necessary.

***N*-(2-Chloro-4-methylquinolin-6-yl)-2-(4-trifluoromethoxyphenoxy)acetamide (13).** The title compound was prepared from 6-amino-2-chlorolepidine (**12**, 4.33 g, 22.4 mmol) and 4-trifluoromethoxyphenoxyacetyl chloride (5.72 g, 22.4 mmol) according to general procedure VII to give 8.72 g (95%) of the pure title compound as a white solid: mp 197–198 °C; ¹H NMR (DMSO-*d*₆) δ 2.62 (s, 3H), 4.84 (s, 2H), 7.13 (d, *J* = 9.0 Hz, 2H), 7.34 (d, *J* = 9.1 Hz, 2H), 7.91 (d, *J* = 9.2 Hz, 1H), 7.98 (dd, *J* = 9.0, 2.3 Hz, 1H), 8.49 (d, *J* = 1.9 Hz, 1H), 10.55 (s, 1H); ¹³C NMR (DMSO-*d*₆) δ 18.9, 68.2, 113.1, 116.8, 123.4, 123.4, 125.1, 127.9, 129.9, 137.8, 143.1, 144.7, 148.8, 157.5, 167.7; MS ESI⁺ *m/z* 411.0 [M + H]. Anal. (C₁₉H₁₄ClF₃N₂O₃) C, H, N, Cl.

***E*)-*N*-[4-Methyl-2-(4-methylpiperazin-1-yl)quinolin-6-yl]-3-*p*-toluylacrylamide (14).** The title compound was prepared from 4-methyl-2-(4-methylpiperazin-1-yl)-quinolin-6-ylamine (**4b**, 256 mg, 1.0 mmol) and 4-methylcinnamoyl chloride (235 mg, 1.3 mmol) according to general procedure V. The product was recrystallized from MeOH to give 305 mg (76%) of light-yellow needles: mp 264–267 °C; ¹H NMR (CDCl₃) δ 2.37 (s, 6H), 2.56 (“t”, *J* = 5.1 Hz, 4H), 2.57 (s, 3H), 3.75 (“t”, *J* = 5.2 Hz, 4H), 6.55 (d, *J* = 15.5 Hz, 1H), 6.83 (s, 1H), 7.16 (d, *J* = 8.1 Hz, 2H), 7.41 (d, *J* = 7.9 Hz, 2H), 7.49 (dd, *J* = 9.0, 2.3 Hz, 1H), 7.67 (d, *J* = 8.9 Hz, 1H), 7.71 (br s, 1H), 7.74 (d, *J* = 15.4 Hz, 1H), 8.41 (s, 1H); HRMS calcd for C₂₅H₂₈N₄O [M + H] 401.2341, found 401.2362. Anal. (C₂₅H₂₈N₄O) C, H, N.

***E*)-*N*-[2-[(2-Dimethylaminoethyl)methylamino]quinolin-6-yl]-3-*p*-toluylacrylamide (42).** The compound was prepared from *N*²-(2-dimethylaminoethyl)-*N*²-methylquinoline-2,6-diamine (**4d**) and 4-methylcinnamoyl chloride according to general procedure V: ¹H NMR (CDCl₃) δ 2.35 (s, 6H), 2.38 (s, 3H), 2.58 (t, *J* = 7.5 Hz, 2H), 3.20 (s, 3H), 3.80 (t, *J* = 7.5 Hz, 2H), 6.55 (d, *J* = 15.4 Hz, 1H), 6.87 (d, *J* = 9.2 Hz, 1H), 7.19 (d, *J* = 7.9 Hz, 1H), 7.42–7.51 (m, 3H), 7.63 (d, *J* = 9.0 Hz, 1H), 7.74 (d, *J* = 15.6 Hz, 1H), 7.84 (d, *J* = 9.0 Hz, 1H), 8.20 (br s, 1H); HRMS calcd for C₂₄H₂₉N₄O [M + H] 389.2341, found 389.2351.

***E*)-*N*-[2-(4-Ethylpiperazin-1-yl)-3-methylquinolin-6-yl]-3-(4-trifluoromethoxyphenyl)acrylamide (43).** The title compound was prepared from 6-amino-2-(4-ethylpiperazin-1-yl)-3-methylquinoline (**4g**) and 4-trifluoromethoxycinnamoyl chloride according to general procedure V: MS ESI⁺ *m/z* 484.9 [M + H]; HPLC (A1) >99%, (B1) 98%.

***E*)-*N*-[2-[(2-Dimethylaminoethyl)methylamino]-4-ethylquinolin-6-yl]-3-(4-trifluoromethoxyphenyl)acrylamide (45).** The title compound was prepared from *N*²-(2-dimethylaminoethyl)-4-ethyl-*N*²-methylquinoline-2,6-diamine (**4i**, 100 mg, 0.37 mmol) and 4-trifluoromethoxycinnamoyl chloride (93 mg, 0.37 mmol) according to general procedure V and purified by solid-phase extraction (SCX column, CH₂Cl₂ → MeOH → MeOH with 5% NH₄OH) to give 96 mg (53%) of yellow solid: ¹H NMR (CDCl₃) δ 1.35 (d, *J* = 7.5 Hz, 3H), 2.34 (s, 6H), 2.57 (t, *J* = 7.3 Hz, 2H), 2.97 (q, *J* = 7.4 Hz, 2H), 3.20 (s, 3H), 3.79 (t, *J* = 7.3 Hz, 2H), 6.59 (d, *J* = 15.6 Hz, 1H), 6.73 (s, 1H), 7.18 (d, *J* = 8.7 Hz, 2H), 7.51 (m, 3H), 7.64 (d, *J* = 9.1 Hz, 1H), 7.74 (d, *J* = 15.4 Hz, 1H), 7.86 (br s, 1H), 8.42 (s, 1H); HRMS calcd for C₂₆H₃₀F₃N₄O₂ [M + H] 487.2321, found 487.2312; HPLC (A1) >99%.

***N*-(4-Methyl-2-morpholin-4-ylquinolin-6-yl)-2-(4-trifluoromethoxyphenoxy)acetamide (49).** A solution of 6-amino-4-methyl-2-(4-morpholinyl)quinoline (**4m**, 0.55 g, 2.3 mmol) in CH₂Cl₂ (30 mL) was added dropwise to a solution of 4-trifluoromethoxyphenoxyacetyl chloride (0.64 g, 2.5 mmol) in CH₂Cl₂ (4 mL). The reaction mixture, which quickly became green and turbid, was stirred at room temperature for 3 h, then diluted with CH₂Cl₂ (150 mL). The organic phase was washed with saturated aqueous Na₂CO₃ and brine, dried (MgSO₄), and concentrated. The residue was recrystallized from MeOH to give 567 mg (55%) of woolly white crystals: mp 206–207 °C; ¹H NMR (DMSO-*d*₆) δ 2.52 (s, 3H), 3.60 (m, 4H), 3.72 (m, 4H), 4.78 (s, 2H), 7.12 (m, 2H), 7.13 (s, 1H), 7.33 (m, 2H), 7.55 (d,

$J = 9.0$ Hz, 1H), 7.75 (dd, $J = 8.9, 2.3$ Hz, 1H), 8.20 (d, $J = 2.8$ Hz, 1H), 10.22 (s, 1H); ^{13}C NMR (DMSO- d_6) δ 18.6, 45.1, 66.1, 67.4, 110.4, 113.0, 116.0, 121.8, 122.5, 123.0, 127.0, 132.8, 142.1, 144.1, 144.3, 156.6, 156.7, 166.1; HRMS calcd for $\text{C}_{23}\text{H}_{23}\text{F}_3\text{N}_3\text{O}_4$ [M + H] 462.1641, found 462.1638. Anal. ($\text{C}_{23}\text{H}_{22}\text{F}_3\text{N}_3\text{O}_4$) C, H, N.

2-(2,4-Dichlorophenoxy)-N-(4-methyl-2-piperazin-1-yl)quinolin-6-yl)acetamide (51). The title compound was prepared from *tert*-butyl 4-(6-amino-4-methylquinolin-2-yl)-piperazine-1-carboxylate (**4l**) and 2,4-dichlorophenoxyacetyl chloride according to general procedures V and VI: ^1H NMR (CDCl_3) δ 2.61 (s, 3H), 3.02 ("t", $J = 5.1$ Hz, 4H), 3.70 ("t", $J = 5.1$ Hz, 4H), 4.66 (s, 2H), 6.86 (s, 1H), 6.92 (d, $J = 8.9$ Hz, 1H), 7.26 (dd, $J = 8.9, 2.6$ Hz, 1H), 7.47 (d, $J = 2.5$ Hz, 1H), 7.52 (dd, $J = 8.9, 2.5$ Hz, 1H), 7.70 (d, $J = 8.9$ Hz, 1H), 8.28 (d, $J = 2.3$ Hz, 1H), 8.63 (s, 1H); HRMS calcd for $\text{C}_{22}\text{H}_{23}\text{Cl}_2\text{N}_4\text{O}_2$ [M + H] 445.1198, found 445.1194. Anal. ($\text{C}_{22}\text{H}_{22}\text{Cl}_2\text{N}_4\text{O}_2 \cdot \frac{1}{6}\text{H}_2\text{O}$) C, H, N, Cl.

(E)-N-[2-(cis-3,5-Dimethylpiperazin-1-yl)-4-methylquinolin-6-yl]-2-(4-trifluoromethoxyphenoxy)acetamide (54). The title compound was prepared from *tert*-butyl 4-(6-amino-4-methylquinolin-2-yl)-*cis*-2,6-dimethylpiperazine-1-carboxylate (**4q**) and 4-trifluoromethoxyacetyl chloride according to general procedures V and VI: mp 202–208 °C; ^1H NMR (DMSO- d_6) δ 1.05 (d, $J = 6.0$ Hz, 6H), 2.32 (t, $J = 11.7$ Hz, 2H), 2.53 (s, 3H), 2.77 (m, 2H), 4.36 (d, $J = 11.1$ Hz, 2H), 6.88 (d, $J = 15.8$ Hz, 1H), 7.14 (s, 1H), 7.45 (d, $J = 8.7$ Hz, 2H), 7.54 (d, $J = 8.9$ Hz, 1H), 7.63 (d, $J = 15.6$ Hz, 1H), 7.76 (s, 1H), 7.77 (d, $J = 8.3$ Hz, 2H), 8.26 (d, $J = 1.3$ Hz, 1H), 10.36 (s, 1H); ^{13}C NMR (DMSO- d_6) δ 18.6, 19.3, 50.2, 51.2, 110.6, 112.4, 118.3, 121.4, 121.7, 122.5, 122.8, 123.6, 126.8, 129.5, 133.3, 134.1, 138.1, 144.0, 144.2, 148.9, 156.2, 163.1; HRMS calcd for $\text{C}_{26}\text{H}_{27}\text{F}_3\text{N}_4\text{O}_2$ [M + H] 485.2164, found 485.2169. Anal. ($\text{C}_{26}\text{H}_{27}\text{F}_3\text{N}_4\text{O}_2 \cdot \frac{1}{3}\text{H}_2\text{O}$) C, H, N.

N-[4-Methyl-2-(4-pyrrolidin-1-yl)piperidin-1-yl]quinolin-6-yl]-2-(4-trifluoromethoxyphenoxy)acetamide (56). The 2-chloroquinoline **13** (205 mg, 0.5 mmol) and 4-(1-pyrrolidinyl)piperidine (0.80 g, 5.0 mmol) were mixed and heated by microwaves to 180 °C for 15 min. The resulting mixture was purified by flash chromatography (SiO_2 , MeOH/ CH_2Cl_2 , 1:10 to 1:2) to give 224 mg (94%) of yellow solid: mp ~180 °C (dec); ^1H NMR (DMSO- d_6) δ 1.45 (m, 2H), 1.72 (m, 4H), 1.96 (br d, $J \approx 11.3$ Hz, 2H), 2.51 (s, 3H), 2.68 (m, 4H), 2.96 (t, $J = 11.3$ Hz, 2H), 4.42 (d, $J = 12.4$ Hz, 2H), 4.78 (s, 2H), 7.12 (m, 2H), 7.15 (s, 1H), 7.34 (d, $J = 8.3$ Hz, 2H), 7.52 (d, $J = 9.1$ Hz, 1H), 7.73 (dd, $J = 9.1, 2.3$ Hz, 1H), 8.17 (d, $J = 2.3$ Hz, 1H), 10.23 (d, 1H); ^{13}C NMR (DMSO- d_6) δ 18.6, 22.8, 30.0, 43.2, 50.7, 61.1, 67.4, 110.6, 113.0, 116.0, 120.2 (q, $J_{\text{CF}} = 254$ Hz), 122.5, 122.6, 122.9, 126.8, 132.5, 142.1, 144.2, 144.3, 156.2, 156.7, 166.0; HRMS calcd for $\text{C}_{28}\text{H}_{32}\text{F}_3\text{N}_4\text{O}_3$ [M + H] 529.2427, found 529.2419. Anal. ($\text{C}_{28}\text{H}_{31}\text{F}_3\text{N}_4\text{O}_3 \cdot \frac{3}{4}\text{H}_2\text{O}$) C, H, N.

2-(2,4-Dichlorophenoxy)-N-[2-[(2-dimethylaminoethyl)methylamino]-4-methylquinolin-6-yl]-acetamide (59). The title compound was prepared from 6-amino-2-(dimethylaminoethyl)methylamine-4-methylquinoline (**4c**, 1.02 g, 3.95 mmol) and 2,4-dichlorophenoxyacetyl chloride according to general procedure V. The residue was purified by flash chromatography (SiO_2 , MeOH with 5% NH_4OH)/EtOAc, 1:9 to 1:5) to give 590 mg (32%) of product: ^1H NMR (DMSO- d_6) δ 2.26 (s, 3H), 2.51 (s, 6H), 3.20–3.80 (m, 4H), 3.41 (s, 3H), 4.90 (s, 2H), 6.94 (s, 1H), 7.15 (d, $J = 8.9$ Hz, 1H), 7.40 (dd, $J = 9.0, 2.6$ Hz, 1H), 7.49 (d, $J = 8.9$ Hz, 1H), 7.60–7.70 (m, 2H), 8.16 (d, $J = 2.3$ Hz, 1H), 10.29 (s, 1H); MS ESI⁺ m/z 461.1 [M + H]; HPLC (A1): 97%.

The product was suspended in Et₂O (10 mL), and 2.0 M HCl in Et₂O was added. The turbid mixture was stirred for 30 min, then was concentrated and dried in vacuo to produce 660 mg (31%) of the dihydrochloride salt of the title compound as a white powder: mp 217–221 °C; ^1H NMR (DMSO- d_6) δ 2.64 (s, 3H), 2.84 (s, 6H), 3.35–3.50 (m, 2H), 3.43 (s, 3H), 4.26 (m, 2H), 5.00 (s, 2H), 7.16 (d, $J = 8.9$ Hz, 1H), 7.37 (dd, $J = 9.0, 2.6$ Hz, 1H), 7.61 (d, $J = 2.4$ Hz, 1H), 7.62 (br s, 1H), 7.93 (d, $J = 9.2$ Hz, 1H), 8.41 (s, 1H), 8.44 (br s, 1H), 11.02 (s, 1H),

11.25 (br s, 1H), 13.10 (br s, 1H); HRMS calcd for $\text{C}_{23}\text{H}_{27}\text{Cl}_2\text{N}_4\text{O}_2$ [M + H] 461.1511, found 461.1513. Anal. ($\text{C}_{23}\text{H}_{26}\text{Cl}_2\text{N}_4\text{O}_2 \cdot 2\text{HCl} \cdot \frac{5}{2}\text{H}_2\text{O}$) C, H, N, Cl.

(E)-N-[2-(2-Dimethylaminoethylamino)-4-methylquinolin-6-yl]-3-(4-trifluoromethoxyphenyl)acrylamide (61). The title compound was prepared from *tert*-butyl (2-dimethylaminoethyl){4-methyl-6-[(E)-3-(4-trifluoromethoxyphenyl)acryloylamino]quinolin-2-yl}carbamate (**5a**, 1.20 g, 2.12 mmol) according to general procedure VI. The product was purified by flash chromatography (SiO_2 , CH_2Cl_2 /MeOH/ NH_4OH , 80:20:1) to give 680 mg (70%) of yellow solid: mp 213–215 °C; ^1H NMR (CDCl_3) δ 2.30 (s, 6H), 2.52 (s, 3H), 2.59 (t, $J = 6.0$ Hz, 2H), 3.56 ("q", $J = 5.3$ Hz, 2H), 5.41 (br s, 1H), 6.54 (s, 1H), 6.59 (d, $J = 15.4$ Hz, 1H), 7.22 (d, $J = 8.5$ Hz, 2H), 7.49–7.59 (m, 3H), 7.60–7.71 (m, 2H), 7.75 (d, $J = 15.4$ Hz, 1H), 8.34 (s, 1H); HRMS calcd for $\text{C}_{24}\text{H}_{26}\text{F}_3\text{N}_4\text{O}_2$ [M + H] 459.2008, found 459.1990. Anal. ($\text{C}_{24}\text{H}_{25}\text{F}_3\text{N}_4\text{O}_2 \cdot \frac{1}{4}\text{H}_2\text{O}$) C, H, N.

N-{2-[(1-Ethylpyrrolidin-2-ylmethyl)amino]-4-methylquinolin-6-yl}-2-(4-trifluoromethoxyphenoxy)acetamide (63). To *tert*-butyl (6-amino-4-methylquinolin-2-yl)-(1-ethylpyrrolidin-2-ylmethyl)carbamate (**4s**, 1.34 g, 3.5 mmol) in CH_2Cl_2 (30 mL) were added Et₃N (0.60 mL, 4.3 mmol) and trifluoromethoxyacetyl chloride (0.97 g, 3.8 mmol), and the mixture was stirred at room temperature. After 12 h, TFA (15 mL) was added to the reaction mixture, and stirring at room temperature was continued. After 24 h the reaction mixture was concentrated and the residue was taken up in CH_2Cl_2 . The organic phase was washed with saturated K₂CO₃ and brine and concentrated. The residue was purified by flash chromatography (SiO_2 , MeOH with 5% NH_4OH)/EtOAc, 1:5) to give 422 mg (24%) as a yellow syrup: ^1H NMR (CDCl_3) δ 1.16 (t, $J = 6.8$ Hz, 3H), 1.82 (m, 1H), 1.96 (m, 1H), 2.05–2.41 (m, 4H), 2.54 (s, 3H), 2.80–2.99 (m, 2H), 3.29 (m, 1H), 3.46 (m, 1H), 3.74 (m, 1H), 4.64 (s, 2H), 5.51 (br s, 1H), 6.57 (s, 1H), 7.03 ("d", $J = 9.2$ Hz, 2H), 7.22 ("d", $J = 8.5$ Hz, 2H), 7.55 (d, $J = 8.9$ Hz, 1H), 7.64 (d, $J = 8.9$ Hz, 1H), 8.15 (s, 1H), 8.30 (s, 1H); ^{13}C NMR (CDCl_3) δ 13.8, 19.2, 23.2, 28.7, 42.8, 48.9, 53.8, 54.0, 68.5, 113.4, 114.8, 116.3, 120.7, 123.1, 123.2, 124.2, 127.6, 130.9, 144.8, 146.2, 155.9, 157.4, 165.9.

The mesylate salt was formed by dissolving the free amine in chloroform and adding 1.0 M methylsulfonic acid (1 equiv). The suspension was concentrated to give the highly hygroscopic mesylate salt in quantitative yield: ^1H NMR (DMSO- d_6) δ 1.28 (t, $J = 7.1$ Hz, 3H), 1.85 (m, 2H), 1.99 (m, 1H), 2.14 (m, 1H), 2.33 (s, 3H), 2.48 (s, 3H), 3.10–3.30 (m, 4H), 3.53 (m, 2H), 3.72 (m, 3H), 4.78 (s, 2H), 6.75 (s, 1H), 7.12 ("d", $J = 9.2$ Hz, 2H), 7.34 ("d", $J = 9.0$ Hz, 2H), 7.52 (d, $J = 8.7$ Hz, 1H), 7.53 (s, 1H), 7.81 (d, $J = 9.2$ Hz, 1H), 8.19 (d, $J = 1.9$ Hz, 1H), 10.28 (s, 1H); HRMS calcd for $\text{C}_{26}\text{H}_{30}\text{F}_3\text{N}_4\text{O}_3$ [M + H] 503.2270, found 503.2287. Anal. ($\text{C}_{26}\text{H}_{29}\text{F}_3\text{N}_4\text{O}_3 \cdot \text{CH}_3\text{SO}_3\text{H} \cdot \frac{7}{4}\text{H}_2\text{O}$) C, H, N, S.

2-(2,4-Dichlorophenoxy)-N-[2-(2-dimethylaminoethoxy)-4-methylquinolin-6-yl]acetamide (65). The title compound was prepared from 2-(2-dimethylaminoethoxy)-4-methylquinolin-6-ylamine (**4j**, 1.2 g, 4.9 mmol) and 2,4-dichlorophenoxyacetyl chloride (1.2 g, 5.0 mmol) according to general procedure V. Purification by flash chromatography (SiO_2 , MeOH with 10% NH_4OH)/ CH_2Cl_2 , 1:10) followed by recrystallization from MeOH provided 410 mg (19%) of white solid. The solid was suspended in Et₂O (10 mL), and 2 M HCl in Et₂O (4 mL) was added. The suspension was stirred at room temperature for 12 h, and the solvents were removed in vacuo to provide 517 mg of the dihydrochloride salt: ^1H NMR (DMSO- d_6) δ 2.57 (d, $J = 0.75$ Hz, 3H), 2.85 (d, $J = 4.9$ Hz, 6H), 3.55 (br q, $J = 5.3$ Hz, 2H), 4.72 ("t", $J = 4.5$ Hz, 2H), 4.96 (s, 2H), 6.95 (d, $J = 0.9$ Hz, 1H), 7.15 (d, $J = 9.0$ Hz, 1H), 7.39 (dd, $J = 8.9, 2.5$ Hz, 1H), 7.62 (d, $J = 2.6$ Hz, 1H), 7.76 (d, $J = 8.9$ Hz, 1H), 7.85 (dd, $J = 8.9, 2.1$ Hz, 1H), 8.38 (d, $J = 2.1$ Hz, 1H), 10.39 (br s, 1H), 10.67 (s, 1H); HRMS calcd for $\text{C}_{22}\text{H}_{24}\text{Cl}_2\text{N}_3\text{O}_3$ [M + H] 448.1195, found 448.1194. Anal. ($\text{C}_{22}\text{H}_{23}\text{Cl}_2\text{N}_3\text{O}_3 \cdot 2\text{HCl} \cdot \text{H}_2\text{O}$) C, H, N. HPLC (A2) >99%.

(E)-N-[2-[(2-Hydroxyethyl)methylamino]-4-methylquinolin-6-yl]-3-(4-trifluoromethoxyphenyl)acrylamide (67). To a suspension of **69** (2.3 g, 4.8 mmol) in THF (200 mL) was

added a solution of LiOH·H₂O (405 mg, 9.6 mmol) in water (60 mL), and the solution was stirred at 40 °C for 60 min to give a homogeneous solution. Then it was stirred at room temperature for 12 h. The reaction mixture was concentrated in vacuo to 140 mL, and water was added to form a precipitate that was filtered off and dried in vacuo to afford 1.86 g (89%) of white solid: ¹H NMR (DMSO-*d*₆) δ 2.49 (s, 3H), 3.14 (s, 3H), 3.63 (m, 4H), 4.79 (m, 1H), 4.89 (s, 2H), 6.96 (s, 1H), 7.14 (d, *J* = 9.1 Hz, 1H), 7.39 (dd, *J* = 8.9, 2.6 Hz, 1H), 7.48 (d, *J* = 8.9 Hz, 1H), 7.62 (d, *J* = 2.5 Hz, 1H), 7.63 (dd, *J* = 9.0, 2.4 Hz, 1H), 8.15 (d, *J* = 2.5 Hz, 1H), 10.28 (s, 1H); HRMS calcd for C₂₁H₂₂Cl₂N₃O₃ [M + H] 434.1038, found 434.1045. Anal. (C₂₁H₂₁Cl₂N₃O₃·½H₂O) C, H, N.

General Procedure for Solubility Assessment. The procedure is based on a protocol described by Lipinski et al.³¹ A 10 mM DMSO solution of the compound is added in small increments (first 1 μL, then 5 μL increments), spaced at least 5 min apart, to 1.0 mL of PBS buffer (pH 7.4) at room temperature. The point of appearance of opalescence or precipitate is determined visually. The highest concentration reached, up to 200 μM, without detection of opalescence or precipitation is reported.

Pharmacophore Evaluation and Refinement. Selected benzamide MCH1R antagonists used as the basis for the pharmacophore hypotheses were subjected to conformational analysis by applying a simulated annealing protocol in Cerius2 using the MMFF force field. An initial temperature of 1000 K was used. In the interval 1000–100 K, the temperature was lowered in steps of 100 K. In the interval 100–0 K the temperature was lowered in steps of 10 K. For each temperature, the molecules were optimized in 1000 Monte Carlo steps with minimization (MCM); i.e., each Monte Carlo step was followed by 100 subsequent minimization steps. Each MCM step was accepted or rejected on the basis of the Metropolis criteria. In this way a total of 20 000 MCM steps were applied in the simulated annealing protocol for each molecule. The resulting trajectory was analyzed, and individual conformers were ranked on the basis of their internal energies.

Conversion of Commercial Compound Libraries to Multiconformer Libraries. Electronic catalogues of available compounds from the commercial vendors ChemBridge Research Laboratories (CRL) (257 400 compounds), ChemDiv (338 003 compounds), ComGenex (98 000), InterBioScreen (192 068 compounds), Maybridge (57 046 compounds), and SPECS (148 837 compounds) were obtained, and each compound was transformed by CATALYST (Accelrys, Inc.) into a multiconformational library with a maximum of 255 conformers per molecule and an energy threshold not exceeding 10 kcal/mol of the lowest energy conformation. The first in silico screening round included the CRL, InterBioScreen, and Maybridge libraries, and the following rounds included all vendors.

MCH1R Homology Modeling. The homology modeling study of MCH1R utilized the crystal structure of bovine rhodopsin PDB code 1F88 (solved to 2.8 Å resolution), obtained from the Brookhaven Protein Data Bank, as structural template.^{32,33} The software MODELLER³⁴ was configured to produce 25 three-dimensional comparative homology models of MCH1R. Individual models were evaluated on the basis of manual visualization and MODELLER's fitness score. Further analyses of accessible rotamer states for these residues were conducted within SYBYL³⁵ and the Biopolymer module using the Lovel rotamer library. The docking was performed using the FlexX docking algorithm.³⁶

Conformational Grid Search. The grid conformational search feature within SYBYL³⁵ was used to locate energy minima for the torsional potential around flexible bonds in selected linkers connecting the western aromatic ring with the quinoline. During the grid search, designated bonds were systematically rotated in increments of 10° through the torsion range 0° to 360° followed by 300 conjugated minimization steps. The resulting conformations and associated energies were stored and analyzed to compute the potential energy surface and subsequently to identify the global and local energy minima, their relative energy differences, and associ-

ated energy barriers. The torsion potential around the CH₂–CONH bond of the oxyacetamide linker (–OCH₂CONH–) has a single minimum corresponding to the planar *cis* conformation (0°), and the *trans* conformation (180°) is at the top of a ~10 kcal/mol energy barrier. A search in Relibase (<http://relibase.rutgers.edu>) on the phenoxyacetamide substructure identified the experimental protein–ligand complexes 1ta6, 1mui, 1ldb, 1hpx, 1hiv, 1ivp, 1lee, 1lf2 containing the same linker fragment. All ligands except for 1hiv have a *cis* conformation in their protein-bound form, in agreement with the global minimum of the torsion potential energy surface. The torsion potential energy surface around the CH–CONH bond of the acrylamide linker (–CH=CHCONH–) contains two symmetrical minima close to 40° and 320° and one at 180°, the last favored with 1 kcal/mol. The torsion potential energy surface for CH₂–CONH of the propylamide linker (–CH₂CH₂–CONH–) has three minima, with the global minimum located around 180° favored by ~1 kcal/mol over two symmetric minima corresponding to torsion angles of 80° and 280°.

Transfections and Tissue Culture. The cDNAs encoding the human MCH1R and MCH2R were cloned from a human brain cDNA library and cloned into the eukaryotic expression vectors pcDNA3.1 (Invitrogen) and pIREs (Clontech), respectively. Assays were performed with stably transfected CHO-K1 (Chinese hamster ovary; ATCC no. CCL-61) cells, expressing the human MCH1R or the human MCH2 receptor. Stable MCH1R or MCH2R transfectants of CHO-K1 cells were obtained using 5 μg of plasmid cDNA and a standard calcium phosphate transfection method³⁷ with subsequent selection in 1 mg/mL G418 (Life Technology) for MCH1R and 10 μg/mL Blasticidin (Invitrogen) for MCH2R. Stably transfected CHO-K1 cells were maintained in Ham's F-12 culture medium (Invitrogen) supplemented with 10% (v/v) fetal calf serum (Invitrogen), 100 U/mL penicillin, 100 μg/mL streptomycin (Life Technology), and either 1 mg/mL G418 or 10 μg/mL blasticidin.

Radioligand Binding Assay. Stably transfected CHO-K1 cells, expressing either human MCH1R or human MCH2R, were seeded in multiwell culture plates 1 day before the assay. The number of cells per well was determined by the apparent expression efficiency of the cell line aiming at 5–10% binding of the added radioligand. MCH1R-expressing cells were assayed by competition binding for 3 h at room temperature using 15 pM [¹²⁵I]MCH (Amersham Pharmacia Biotech) plus variable amounts of test compound in 0.5 mL of a 25 mM Hepes buffer, pH 7.4, supplemented with 10 mM MgCl₂, 5 mM MnCl₂, 10 mM NaCl, 0.1% (w/v) bovine serum albumin (BSA), and 100 μg/mL bacitracin. MCH2R expressing cells were assayed by competition binding for 2 h at 37 °C using 30 pM [¹²⁵I]MCH plus variable amounts of test compound in 0.5 mL of a 25 mM Hepes buffer, pH 7.4, supplemented with 5 mM MgCl₂, 10 mM NaCl, 0.1% (w/v) BSA, and 100 μg/mL bacitracin. Assays were performed in duplicate. Nonspecific binding was determined as the binding in the presence of 1 μM MCH (Bachem). Binding data were analyzed and IC₅₀ values determined by nonlinear regression using the Prism software (GraphPad software, San Diego, CA).

Scintillation Proximity Assay (SPA). Measurement of [¹²⁵I]MCH binding was performed in duplicate by incubating membranes and SPA beads with tracer in the presence of various concentrations of test compounds at room temperature for 2 h. Membranes and beads were preincubated for 20 min. The MCH1R binding buffer contained 50 mM Tris (pH 7.4), 8 mM MgCl₂, 12% glycerol, 0.1% (w/v) BSA, and protease inhibitors (complete protease inhibitor cocktail tablet, Roche). A final [¹²⁵I]MCH concentration of 150 pM was applied, and SPA beads (PVT-PEI-WGA type B, RPNQ0004 Amersham Pharmacia Biotech) were used at a final concentration of 0.4 mg/well. Analogously, 5-HT_{2c} competition binding was performed with an SPA assay using [³H]mesulergine (Amersham Pharmacia Biotech) as the radioligand. The 5-HT_{2c} binding buffer contained 50 mM Tris (pH 7.7), 50 mM MgCl₂, and 0.1% pargyline. SPA beads (YSi-WGA, RPNQ0011 Amersham Pharmacia Biotech) were used at a final concentration of 0.4 mg/

well. Nonspecific binding was determined as the binding in the presence of 1 μ M cold mesulergine.

Membranes prepared from CHO-K1 cells expressing either the hMCH1R or the h5-HT_{2c} receptor were purchased from Euroscreen (ES-370-M or ES-315-M, respectively), and a final concentration of 2 μ g/well (hMCH1R) or 4 μ g/well (h5-HT_{2c}) was used. Binding data were analyzed and IC₅₀ values determined by nonlinear regression using the Prism software (GraphPad software, San Diego, CA).

Phosphatidylinositol Assay. Stably transfected CHO-K1 cells, expressing human MCH1R (2 × 10⁵ cells/well), were incubated overnight with 5 μ Ci of [³H]myoinositol (Amersham Pharmacia Biotech). Phosphatidylinositol turnover was stimulated by submaximal concentrations of MCH, i.e., 10 nM, in the presence of increasing amounts of test compound. The test compound was added 5 min before addition of the agonist (MCH). Incubation was in HBSS (Hanks' balanced salt solution) supplemented with 10 mM LiCl at 37 °C for 45 min. Cells were lysed with 10 mM ice-cold formic acid, and the generated [³H]inositol phosphates were purified on Bio-Rad AG 1-X8 anion-exchange resin. Determinations were made in duplicate. Data were analyzed and IC₅₀ values determined by nonlinear regression using the Prism software (GraphPad software, San Diego, CA).

[³⁵S]GTP γ S SPA Binding Assay. Schild analysis was conducted with a [³⁵S]GTP γ S SPA binding assay. The assay was performed by incubating 5 μ g/well hMCH1R membranes (Euroscreen) and 0.4 mg/well SPA beads (PVT-WGA, RP-NQ0001 Amersham Pharmacia Biotech) with 1 nM [³⁵S]GTP γ S (Perkin-Elmer, NEG 030H) in the presence of various concentrations of MCH and test compounds at room temperature for 1 h. The assay buffer contained 50 mM HEPES (pH 7.5), 100 mM NaCl, 5 mM MgCl₂, 0.1% BSA, 3 μ M GDP, and 10 μ g/mL saponin. Dose ratios calculated from EC₅₀ values from MCH concentration response curves were utilized to prepare Schild plots and predict K_B values: compound **59**, K_B = 5.0 ± 1.0 nM; compound **65**, K_B = 76 nM; compound **67**, K_B = 3.0 nM.

Acknowledgment. The authors thank Bo Aastrup, Rokhsana Andersen, Ann Christensen, Joan Gredal, Stina Hansen, and Helle Iversen for valuable discussions and excellent technical assistance.

Supporting Information Available: Purity of central target compounds determined by elemental analysis and/or HPLC, synthetic details, yields, and characterization (mp, ¹H NMR, ¹³C NMR, and/or ESI-MS) for intermediates **1b**, **2a–k**, **3a–q**, **4a–v**, and **5a,b** and target compounds **22**, **26**, **38–41**, **44**, **46–48**, **50**, **52**, **53**, **55**, **57**, **58**, **60**, **62**, **64**, **66**, **68**, and **69**, and coordinates and weights for pharmacophore hypotheses. This material is available free of charge via the Internet at <http://pubs.acs.org>.

References

- (1) (a) Kopelman, P. G. Obesity as a medical problem. *Nature* **2000**, *404*, 635–643. (b) International Association for the Study of Obesity (IASO) (<http://www.iaso.org>).
- (2) (a) Bray, G. A.; Tartaglia, L. A. Medicinal strategies in the treatment of obesity. *Nature* **2000**, *404*, 672–677. (b) Fernández-López, J.-A.; Remesar, X.; Foz, M.; Alemany, M. Pharmacological approaches for the treatment of obesity. *Drugs* **2002**, *62*, 915–944. (c) Astrup, A. Treatment of Obesity. In *International Textbook of Diabetes Mellitus*, 3rd ed.; DeFronzo, R. A., Ferrannini, E., Keen, H., Zimmet, P., Eds.; John Wiley & Sons: Chichester, U.K., 2004; pp 673–690.
- (3) (a) Schwartz, M. W.; Woods, S. C.; Porte, D., Jr.; Seeley, R. J.; Baskin, D. G. Central nervous system control of food intake. *Nature* **2000**, *404*, 661–671. (b) Dhillon, W. S.; Bloom, S. R. Hypothalamic peptides as targets for obesity. *Curr. Opin. Pharmacol.* **2001**, *1*, 651–655. (c) Largent, B. L.; Robichaud, A. J.; Miller, K. J. Promise and progress of central G protein-coupled receptor modulators for obesity treatments. *Ann. Rep. Med. Chem.* **2002**, *37*, 1–10.
- (4) Reviews: (a) Forray, C. The MCH receptor family: feeding brain disorders? *Curr. Opin. Pharmacol.* **2003**, *3*, 85–89. (b) Hervieu, G. Melanin-concentrating hormone functions in the nervous system: food intake and stress. *Expert Opin. Ther. Targets* **2003**, *7*, 495–511. (c) Kawano, H.; Honma, S.; Honma, A.; Horie, M.; Kawano, Y.; Hayashi, S. Melanin-concentrating hormone neuron system: the wide web that controls the feeding. *Anat. Sci. Int.* **2002**, *77*, 149–160. (d) Butler, A. A.; Cone, R. D. Knockout models resulting in the development of obesity. *Trends Genet.* **2001**, *17*, S50–S53.
- (5) (a) Presse, F.; Sorokovsky, I.; Max, J.-P.; Nicolaidis, S.; Nahon, J.-L. Melanin-concentrating hormone is a potent anorectic peptide regulated by food-deprivation and glucopenia in the rat. *Neuroscience* **1996**, *71*, 735–745. (b) Qu, D.; Ludwig, D. S.; Gammeltoft, S.; Piper, M.; Pellemounter, M. A.; Cullen, M. J.; Mathes, W. F.; Przypek, J.; Kanarek, R.; Maratos-Flier, E. A role for melanin-concentrating hormone in the central regulation of feeding behaviour. *Nature* **1996**, *380*, 243–247. (c) Rossi, M.; Choi, S. J.; O'Shea, D.; Miyoshi, T.; Ghatel, M. A.; Bloom, S. R. Melanin-concentrating hormone acutely stimulates feeding, but chronic administration has no effect on body weight. *Endocrinology* **1997**, *138*, 351–355.
- (6) Shimada, M.; Tritos, N. A.; Lowell, B. B.; Flier, J. S.; Maratos-Flier, E. Mice lacking melanin-concentrating hormone are hypophagic and lean. *Nature* **1998**, *396*, 670–674.
- (7) Ludwig, D. S.; Tritos, N. A.; Mastaitis, J. W.; Kulkarni, R.; Kokkotou, E.; Elmquist, J.; Lowell, B.; Flier, J. S.; Maratos-Flier, E. Melanin-concentrating hormone overexpression in transgenic mice leads to obesity and insulin resistance. *J. Clin. Invest.* **2001**, *107*, 379–386.
- (8) (a) Monzon, M. E.; de Souza, M. M.; Izquierdo, L. A.; Izquierdo, I.; Barros, D. M.; de Barioglio, S. R. Melanin-concentrating hormone (MCH) modifies memory retention in rats. *Peptides* **1999**, *20*, 1517–1519. (b) Varas, M.; Perez, M.; Monzon, M. E.; Rubiales de Barioglio, S. Melanin-concentrating hormone, hippocampal nitric oxide levels and memory retention. *Peptides* **2002**, *23*, 2213–2221.
- (9) (a) Monzon, M. E.; De Barioglio, S. R. Response to novelty after i.c.v. injection of melanin-concentrating hormone (MCH) in rats. *Physiol. Behav.* **1999**, *67*, 813–817. (b) Kela, J.; Salmi, P.; Rimondini-Giorgini, R.; Heilig, M.; Wahlestedt, C. Behavioural analysis of melanin-concentrating hormone in rats: evidence for orexigenic and anxiolytic properties. *Regul. Pept.* **2002**, *114*, 109–114.
- (10) Borowsky, B.; Durkin, M. M.; Ogozalek, K.; Marzabadi, M. R.; DeLeon, J.; Heurich, R.; Lichtblau, H.; Shaposhnik, Z.; Daniewska, I.; Blackburn, T. P.; Branchek, T. A.; Gerald, C.; Vaysse, P. J.; Forray, C. Antidepressant, anxiolytic and anorectic effects of a melanin-concentrating hormone-1 receptor antagonist. *Nat. Med.* **2002**, *8*, 825–830.
- (11) Identification of MCH1R: (a) Chambers, J.; Ames, R. S.; Bergsma, D.; Muir, A.; Fitzgerald, L. R.; Hervieu, G.; Dytko, G. M.; Foley, J. J.; Martins, J.; Liu, W.-S.; Park, J.; Ellis, C.; Ganguly, S.; Konchar, S.; Cluderay, J.; Leslie, R.; Wilson, S.; Sarau, H. M. Melanin-concentrating hormone is the cognate ligand for the orphan G protein-coupled receptor SLC-1. *Nature* **1999**, *400*, 261–265. (b) Saito, Y.; Nothacker, H.-P.; Wang, Z.; Lin, S. H. S.; Leslie, F.; Civelli, O. Molecular characterization of the melanin-concentrating-hormone receptor. *Nature* **1999**, *400*, 265–269.
- (12) Identification of MCH2R: (a) Sailer, A. W.; Sano, H.; Zeng, Z.; McDonald, T. P.; Pan, J.; Pong, S.-S.; Feighner, S. D.; Tan, C. P.; Fukami, T.; Iwaasa, H.; Hreniuk, D. L.; Morin, N. R.; Sadowski, S. J.; Ito, M.; Ito, M.; Bansal, A.; Ky, B.; Figueroa, D. J.; Jiang, Q.; Austin, C. P.; MacNeil, D. J.; Ishihara, A.; Ihara, M.; Kanatani, A.; Van der Ploeg, L. H. T.; Howard, A. D.; Liu, Q. Identification and characterization of a second melanin-concentrating hormone receptor, MCH-2R. *Proc. Natl. Acad. Sci. U.S.A.* **2001**, *98*, 7564–7569. (b) An, S.; Cutler, G.; Zhao, J. J.; Huang, S.-G.; Tian, H.; Li, W.; Liang, L.; Rich, M.; Bakleh, A.; Du, J.; Chen, J.-L.; Dai, K. Identification and characterization of a melanin concentrating hormone receptor. *Proc. Natl. Acad. Sci. U.S.A.* **2001**, *98*, 7576–7581.
- (13) Marsh, D. J.; Weingarh, D. T.; Novi, D. E.; Chen, H. Y.; Trumbauer, M. E.; Chen, A. S.; Guan, X.-M.; Jiang, M. M.; Feng, Y.; Camacho, R. E.; Shen, Z.; Frazier, E. G.; Yu, H.; Metzger, J. M.; Kuca, S. J.; Shearman, L. P.; Gopal-Truter, S.; MacNeil, D. J.; Strack, A. M.; MacIntyre, D. E.; Van der Ploeg, L. H. T.; Qian, S. Melanin-concentrating hormone 1 receptor-deficient mice are lean, hyperactive, and hyperphagic and have altered metabolism. *Proc. Natl. Acad. Sci. U.S.A.* **2002**, *99*, 3240–3245.
- (14) Takekawa, S.; Asami, A.; Ishihara, Y.; Terauchi, J.; Kato, K.; Shimomura, Y.; Mori, M.; Murakoshi, H.; Kato, K.; Suzuki, N.; Nishimura, O.; Fujino, M. T-226296: a novel, orally active and selective melanin-concentrating hormone receptor antagonist. *Eur. J. Pharmacol.* **2002**, *438*, 129–135.
- (15) (a) Bednarek, M. A.; Hreniuk, D. L.; Tan, C.; Palyha, O. C.; MacNeil, D. J.; Van der Ploeg, L. H. Y.; Howard, A. D.; Feighner, S. D. Synthesis and biological evaluation in vitro of selective, high affinity peptide antagonists of human melanin-concentrating hormone action at human melanin-concentrating hormone receptor 1. *Biochemistry* **2002**, *41*, 6383–6390. (b) Shearman,

- L. P.; Camacho, R. E.; Stribling, D. S.; Zhoua, D.; Bednarek, M. A.; Hreniuk, D. L.; Feighner, S. D.; Tan, C. P.; Howard, A. D.; Van der Ploeg, L. H. T.; MacIntyre, D. E.; Hickey, G. J.; Strack, A. M. Chronic MCH-1 receptor modulation alters appetite, body weight and adiposity in rats. *Eur. J. Pharmacol.* **2003**, *475*, 37–47. Note: the peptide sequence for the antagonist (compound B) is erroneous in ref 15b; the correct one is given in ref 15a.
- (16) (a) Souers, A. J.; Gao, J.; Brune, M.; Bush, E.; Wodka, D.; Vasudevan, A.; Judd, A. S.; Mulhern, M.; Brodjian, S.; Dayton, B.; Shapiro, R.; Hernandez, L. E.; Marsh, K. C.; Sham, H. L.; Collins, C. A.; Kym, P. R. Identification of 2-(4-benzyloxyphenyl)-N-[1-(2-pyrrolidin-1-yl-ethyl)-1H-indazol-6-yl]acetamide, an orally efficacious melanin-concentrating hormone receptor 1 antagonist for the treatment of obesity. *J. Med. Chem.* **2005**, *48*, 1318–1321. (b) McBriar, M. D.; Guzik, H.; Xu, R.; Paruchova, J.; Li, S.; Palani, A.; Clader, J. W.; Greenlee, W. J.; Hawes, B. E.; Kowalski, T. J.; O'Neill, K.; Spar, B.; Weig, B. Discovery of bicycloalkyl urea melanin concentrating hormone receptor antagonists: orally efficacious antiobesity therapeutics. *J. Med. Chem.* **2005**, *48*, 2274–2277.
- (17) (a) Receveur, J.-M.; Bjurling, E.; Ulven, T.; Little, P. B.; Nørregaard, P. K.; Högberg, T. 4-Acylamino- and 4-ureidobenzamides as melanin-concentrating hormone (MCH) receptor 1 antagonists. *Bioorg. Med. Chem. Lett.* **2004**, *14*, 5075–5080. (b) Högberg, T.; Bjurling, A. E.; Receveur, J.-M.; Little, P. B.; Elling, C. E.; Nørregaard, P. K.; Ulven, T. Novel methoxybenzamide compounds for use in MCH receptor related disorders. Int. Pat. Appl. WO 03/087045 A1, 2003.
- (18) (a) The term *physicogenetic* refers to a method for classifying receptors by comparing physicochemical properties of the binding site amino acid residues and thereby identifying the receptors most likely to bind similar ligands, as opposed to conventional *phylogenetic* classification comparing homologies of the entire protein sequence. (b) Frimurer, T.; Ulven, T.; Elling, C.; Gerlach, L.-O.; Högberg, T. A physicogenetic method to assign ligand-binding relationships between 7TM receptors applied on CRTH2. *Drugs Future* **2004**, *29* (Suppl. A), 79 (18th International Symposium on Medicinal Chemistry). (c) Frimurer, T. M.; Ulven, T.; Elling, C. E.; Gerlach, L.-O.; Kostenis, E.; Högberg, T. A physicogenetic method to assign ligand-binding relationships between 7TM Receptors. *Bioorg. Med. Chem. Lett.* **2005**, *15*, 3707–3712.
- (19) (a) Högberg, T. The development of dopamine D₂-receptor selective antagonists. *Drug Design Discovery* **1993**, *9*, 333–350. (b) Högberg, T.; Norinder, U.; Råmsby, S.; Stensland, B. Crystallographic, theoretical and molecular modeling studies on the conformations of the salicylamide, raclopride, a selective dopamine-D₂ antagonist. *J. Pharm. Pharmacol.* **1987**, *39*, 787–796.
- (20) (a) Frimurer, T. M. Unpublished results. (b) Recently a corroborating study on a simulated complex of the aminotetraline T-226296 with MCH1R has been published: Vitale, R. M.; Pedone, C.; De Benedetti, P. G.; Fanelli, F. Structural features of the inactive and active states of the melanin-concentrating hormone receptors: insights from molecular simulations. *Proteins* **2004**, *56*, 430–448.
- (21) Frimurer, T. M.; Ulven, T.; Högberg, T.; Nørregaard, P. K.; Little, P. B.; Receveur, J.-M. Quinoline compounds for use in MCH receptor related disorders. Int. Pat. Appl. WO 04/052370 A2, 2004.
- (22) (a) Clark, D. E.; Higgs, C.; Wren, S. P.; Dyke, H. J.; Wong, M.; Norman, D.; Lockey, P. M.; Roach, A. G. A virtual screening approach to finding novel and potent antagonists at the melanin-concentrating hormone 1 receptor. *J. Med. Chem.* **2004**, *47*, 3962–3971. (b) Arienzo, R.; Clark, D. E.; Cramp, S.; Daly, S.; Dyke, H. J.; Lockey, P.; Norman, D.; Roach, A. G.; Stuttle, K.; Tomlinson, M.; Wong, M.; Wren, S. P. Structure–activity relationships of a novel series of melanin-concentrating hormone (MCH) receptor antagonists. *Bioorg. Med. Chem. Lett.* **2004**, *14*, 4099–4102.
- (23) (a) Devita, R. J.; Chang, L.; Chung, D.; Hoang, M.; Jiang, J.; Lin, P.; Sailer, A. W.; Young, J. R. 2-Aminoquinoline compounds. Int. Pat. Appl. WO 03/045313 A2, 2003. (b) Devita, R. J.; Chang, L.; Hoang, M.; Jiang, J.; Lin, P.; Sailer, A. W. 4-Aminoquinoline compounds. Int. Pat. Appl. WO 03/045920 A1, 2003.
- (24) (a) Souers, A. J.; Wodka, D.; Gao, J.; Lewis, J. C.; Vasudevan, A.; Gentles, R.; Brodjian, S.; Dayton, B.; Ogiela, C. A.; Fry, D.; Hernandez, L. E.; Marsh, K. C.; Collins, C. A.; Kym, P. R. Synthesis and evaluation of 2-amino-8-alkoxy quinolines as MCHr1 antagonists. Part 1. *Bioorg. Med. Chem. Lett.* **2004**, *14*, 4873–4877. (b) Vasudevan, A.; Wodka, D.; Verzal, M. K.; Souers, A. J.; Gao, J.; Brodjian, S.; Fry, D.; Dayton, B.; Marsh, K. C.; Hernandez, L. E.; Ogiela, C. A.; Collins, C. A.; Kym, P. R. Synthesis and evaluation of 2-amino-8-alkoxy quinolines as MCHr1 antagonists. Part 2. *Bioorg. Med. Chem. Lett.* **2004**, *14*, 4879–4882. (c) Souers, A. J.; Wodka, D.; Gao, J.; Lewis, J. C.; Vasudevan, A.; Brodjian, S.; Dayton, B.; Ogiela, C. A.; Fry, D.; Hernandez, L. E.; Marsh, K. C.; Collins, C. A.; Kym, P. R. Synthesis and evaluation of 2-amino-8-alkoxy quinolines as MCHr1 antagonists. Part 3. *Bioorg. Med. Chem. Lett.* **2004**, *14*, 4883–4886.
- (25) *Catalyst 4.7*; Accelrys, Inc. 10188 Telesis Court, Suite 100, San Diego, CA 92121; www.accelrys.com.
- (26) (a) Frimurer, T. M.; Peters, G. H.; Iversen, L. F.; Andersen, H. S.; Møller, N. P.; Olesen, O. H. Ligand-induced conformational changes: improved predictions of ligand binding conformations and affinities. *Biophys. J.* **2003**, *84*, 2273–2281. (b) Stultz, C. M.; Karplus, M. Dynamic ligand design and combinatorial optimization. *Proteins: Struct., Funct., Genet.* **2000**, *40*, 258–289.
- (27) Krahler, S. E.; Burger, A. Cyclic aminoalkylamino derivatives of lepidine. *J. Am. Chem. Soc.* **1941**, *63*, 2367–2371.
- (28) Johnson, O. H.; Hamilton, C. S. Syntheses in the quinoline series. III. The nitration of 2-chloro-4-methylquinoline and the preparation of some 2-hydroxy-4-methyl-8-(dialkylaminoalkyl)-aminoquinolines. *J. Am. Chem. Soc.* **1941**, *63*, 2867–2869.
- (29) (a) Bickerdike, M. J. 5-HT_{2C} receptor agonists as potential drugs for the treatment of obesity. *Curr. Top. Med. Chem.* **2003**, *3*, 885–897. (b) Hayashi, A.; Sonoda, R.; Kimura, Y.; Takasu, T.; Suzuki, M.; Sasamata, M.; Miyata, K. Antiobesity effect of YM348, a novel 5-HT_{2C} receptor agonist, in Zucker rats. *Brain Res.* **2004**, *1011*, 221–227.
- (30) The pK_a calculations were performed with the on-line calculator SPARC: <http://ibmlc2.chem.uga.edu/sparc/>.
- (31) Lipinski, C. A.; Lombardo, F.; Dominy, B. W.; Feeney, P. J. Experimental and computational approaches to estimate solubility and permeability in drug discovery and development settings. *Adv. Drug Delivery Rev.* **1997**, *23*, 3–25.
- (32) Palczewski, K.; Kumasaka, T.; Hori, T.; Behnke, C. A.; Motoshima, H.; Fox, B. A.; Le Trong, I.; Teller, D. C.; Okada, T.; Stenkamp, R. E.; Yamamoto, M.; Miyano, M. Crystal structure of rhodopsin: A G protein-coupled receptor. *Science* **2000**, *289*, 739–745.
- (33) Bernstein, F. C.; Koetzle, T. F.; Williams, G. J. B.; Meyer, E. F.; Brice, M. D.; Rogers, J. R.; Kennard, O.; Shimanouchi, T.; Tasumi, M. The Protein Data Bank: a computer based archival file for macromolecular structure. *J. Mol. Biol.* **1997**, *112*, 535–542.
- (34) (a) Marti-Renom, M. A.; Stuart, A.; Fiser, A.; Sánchez, R.; Melo, F.; Sali, A. Comparative protein structure modeling of genes and genomes. *Annu. Rev. Biophys. Biomol. Struct.* **2000**, *29*, 291–325. (b) Sali, A.; Blundell, T. L. Comparative protein modelling by satisfaction of spatial restraints. *J. Mol. Biol.* **1993**, *234*, 779–815. (c) Fiser, A.; Do, R. K.; Sali, A. Modeling of loops in protein structures. *Protein Sci.* **2000**, *9*, 1753–1773.
- (35) SYBYL 7.0; Tripos Inc. (1699 South Hanley Road, St. Louis, MO, 63144).
- (36) Rarey, M.; Kramer, B.; Lengauer, T. Docking of hydrophobic ligands with interaction-based matching algorithms. *Bioinformatics* **1999**, *15*, 243–250.
- (37) (a) Gether, U.; Marray, T.; Schwartz, T. W.; Johansen, T. E. Stable expression of high affinity NK1 (substance P) and NK2 (neurokinin A) receptors but low affinity NK3 (neurokinin B) receptors in transfected CHO cells. *FEBS Lett.* **1992**, *296*, 241–244. (b) Johansen, T. E.; Schøller, M. S.; Tolstoy, S.; Schwartz, T. W. Biosynthesis of peptide precursors and protease inhibitors using new constitutive and inducible eukaryotic expression vectors. *FEBS Lett.* **1990**, *267*, 289–294.

JM050103Y